An-Najah National University

Faculty of Graduate Studies

Combined effects of pressure, temperature, and magnetic field on energy states of donor impurities in a GaAs/AlGaAs quantum heterostructure

By

Samah Fayez Nemer Abu-Zaid

Supervisor

Prof. Mohammad Elsaid

This Thesis is Submitted in Partial Fulfillment of the Requirements for the Degree of Master of Physics, Faculty of Graduate Studies, An-Najah National University, Nablus, Palestine.

2017

Combined effects of pressure, temperature, and magnetic field on energy states of donor impurities in a GaAs/AlGaAs quantum heterostructure

By

Samah Fayez Nemer Abu-Zaid

This thesis was defended successfully on 19\10\2017 and approved by:

Defense committee members	**Signature**
– **Prof. Mohammad Khalil Elsaid / Supervisor**	.....
– **Prof. Jihad Hasan Jabali Asad / External examiner**	.....
– **Prof. Khaled Faisal Ilaiwi / Internal examiner**	.....

Dedication

For my wonderful family for their love, care and support.

Acknowledgments

Firstly, my great thanks to Allah, who with me and help me to complete my thesis and in each moment in my life.

Then, my great thanks go to my advisor and instructor Prof. Dr. Mohammed Elsaid for his guidance, assistance, supervision and contribution of valuable suggestions. And I would like to thank my partners and colleagues in physics department for supporting and helping and I can't forget to thank Ayham Shaer for his help.

I want to take the opportunity to say thanks to my especial family wonderful friends, my work manager and colleagues, and my great students for their moral support and care until the end.

الإقرار

أنا الموقع أدناه مقدم الأطروحة التي تحمل عنوان

Combined effects of pressure, temperature, and magnetic field on energy states of donor impurities in a GaAs/AlGaAs quantum heterostructure

أقر بأن ما اشتملت عليه هذه الرسالة إنما هو نتاج جهدي الخاص، باستثناء ما تمت الإشارة إليه حيثما ورد وأن هذه الرسالة ككل أو جزء منها لم يقدم من قبل لنيل أية درجة أو بحث علمي أو بحثي لدى أية مؤسسة تعليمية أو بحثية أخرى

Declaration

The work provided in this thesis, unless otherwise referenced, is the researcher's own work, and has not been submitted elsewhere for any other degree or qualification.

Student's name:	Samah Fayez Nemer Abu-Zaid	**اسم الطالب :**
Signature:	Samah Abu-Zaid	**التوقيع :**
Date:	19\10\2017	**التاريخ :**

Table of Contents

List of Figures

List of Tables

List of Symbols and Abbreviations

QD	Quantum dot
3D	Three dimension
2D	Two dimension
1D	One dimension
0D	Zero dimension (quantum dot)
nm	Nanometer
DOS	The density of state
ω_o	Confining frequency
ω_c	Cyclotron frequency
γ	Magnetic field strength
B	Magnetic field
GaAs	Gallium Arsenide
AlGaAs	Aluminum Gallium Arsenide
e	Charge of electron
m	Mass of electron
m^*	Effective mass of electron
$\vec{p}(r)$	The linear momentum
$\overrightarrow{A(r)}$	Vector potential
c	Speed of light
ϵ	The dielectric constant of material
R^*	Effective Rydberg unit
$\hbar$	Reduced Blank's constant
α	Effective frequency
∇	Gradient operator
i	Imaginary number
Ψ	Wave function
K	Kelvin Degree
T	Temperature
n	Principle quantum number
m	Angular quantum number
ρ	Position of the electron inside the heterostructure

Combined effects of pressure, temperature, and magnetic field on energy states of donor impurities in a GaAs/AlGaAs quantum heterostructure

By
Samah Fayez Nemer Abu-Zaid
Supervisor
Prof. Mohammad Elsaid

Abstract

The ground state energy of shallow donor impurity in GaAs/AlGaAs heterostructure with an applied magnetic field along z direction, using exact diagonalization method, had been calculated. The effects of the impurity distance on the ground state energy versus the confining frequency and magnetic field strength had been investigated. The impurity binding energy of the ground state had been calculated as a function of impurity position, confining frequency and magnetic field strength. In addition, the combined effects of pressure and temperature, on the binding energy as a function of magnetic field strength had been studied using the effective-mass approximation. The result is that, the donor impurity binding energy enhances with increasing the pressure while it decreases as the temperature decreases.

Chapter One

Introduction

1.1 Quantum Heterostructure

The optical, electrical, and transport properties of the semiconductor materials are sensitive to many effects like applied electric field, applied magnetic field, pressure, temperature, impurity presence and it's position. The semiconductor heterostructure is a nano-material scale which typically varies between 1-100 nm ranges. The donor impurity in a semiconductor system with applied magnetic field form the interesting problem to study for all semiconductor structure from the quantum bulk (3D) up to quantum dot (QD) (the zero dimension 0D), where the donor binding energy enhances as the dimensionality of the heterostructure decreases [1-3]. The change in the density of states (DOS) of the heterostructure, for the QD shows as repeated delta function unlike continuous behavior for 3D, 2D, 1D quantum well wire (QWWs) systems [4].

Donor impurity in a quantum bulk makes change in optical and electrical properties because of the effective charge and effective mass addition to the system. The energy gap of the quantum bulk system change due to the small impurity binding energy and the coulombic interaction between the bulk charge carrier (electron) with the donor impurity [5-6].

Reducing the dimensionality from 3D to 2D cause the quantum well (QW), alter the electrical, optical, transport properties. The donor impurity binding

energy depends significantly on the quantum well layer thickness, impurity position, quantum well QW shape and width. In particular the binding energy of the donor impurity had been calculated as a function of well width and the impurity position [1, 7-8]. The effects of the applied electric field on the donor impurity binding energy, which is known as Stark effect, had been studied [9].

The low dimensional structures (quantum well-wire (QWW) and quantum dot (QD)), can be obtained it by continuous reducing of the dimensionality of the electron movement space, and this fabricated by applying additional confinement potential on the 2D structure to confine the electron to move in a plan. Investigation of this system forms the interesting problem due to its special properties which are varying by changing the radius of the QWW and QD [10, 11]. The presence of the impurity can alter the performance of the quantum devices and the transport properties. As a quasi two dimension structure, the QWW has important advantage which is the high mobility transistor. The optical properties of the QW, QWWs, and QD show a significant dependence on the dimensionality of the nano system [12-13]. The importance of study the quantum dots comes from its applications, where it make the laser production with wave length that hard or impossible to achieve in previous time. In addition, QD has many applications in the solar cell, quantum computer, and single electron transistor [14].

Different studies of the donor impurity located in the low-dimensional structure had been carried. The donor impurity ionization energy affected

by a high magnetic field, where the ionization energy increasing with it [15]. The binding energy of a hydrogenic impurity in InSb/GaAs semiconductor materials with the presence of parallel magnetic field to the QWW axis has been obtained as a function magnetic field strength, wire radius, and the location of the donor impurity from the QWW axis [16]. In addition, the most interesting phenomena are to study the effect of the temperature and pressure on the donor impurity binding energy in reduced dimensions [17].

The great potential of the modern nanotechnology used to produce the zero dimensional structure QD (electron confined in all direction) using different methods like etching and molecular beam epitaxy [18]. The effect of the strong electron confinement in a nano structure leads to a small energy separation between the subbands; increase the dipole transition value [19].

The donor impurity binding energy increases continuously as the QD size decreases; also it depends on the donor impurity position [20]. Increasing the applied magnetic field will increases the binding energy of the donor shallow impurity in a plane and reduces the polarizability. The electrical and optical properties of the impurities for different QD shape (homogenous and inhomogenous QD) are strongly affected by the presence of the donor impurity [21].

In this work we will focus on the heterostructure with impurity nearby in the presence of applied magnetic field, where the electron interacts with the impurity ion located along the vertical z-axis direction by Coulomb

potential, taking into consideration the effects of the pressure and temperature on the GaAs/AlGaAs material parameters: the effective mass and dielectric constant.

1.2 Heterostructure and confinement potential

Consider the heterostructure in the x-y plane with the impurity in the z axis at the distance (0, 0, d), with a uniform external magnetic field of strength B which applied along the z direction, as illustrated in figure 1.1.

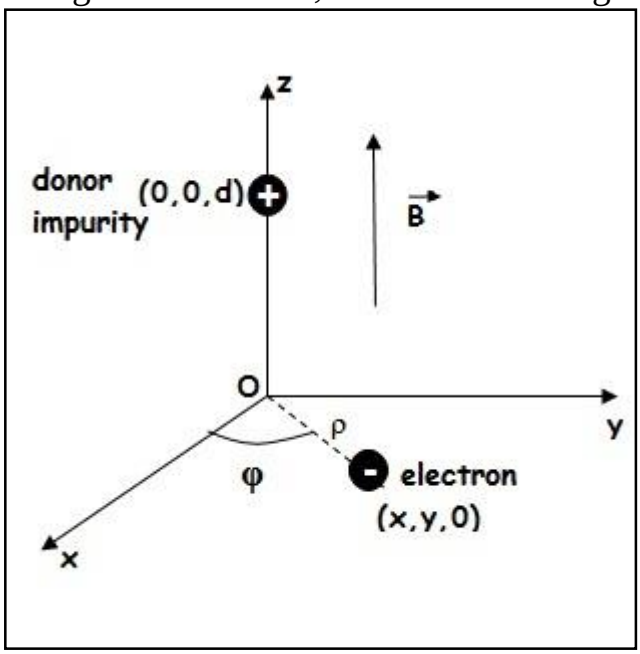

Figure (1.1): An electron at position $\vec{\boldsymbol{\rho}}$ confined in the x y- plane interacting with a positive donor impurity located at position $\vec{\boldsymbol{d}} = \boldsymbol{d}\,\hat{\boldsymbol{k}}$ along z axis and subject to a uniform magnetic field along the growth axis $\vec{\boldsymbol{B}} = \boldsymbol{B}\,\hat{\boldsymbol{k}}$.

The structure of this system is sketched in figure 1.2, which includes two AlGaAs layers separated by GaAs layer, one of the AlGaAs layer doped with donor impurity located at distance (d) along the growth axis.

AlGaAs used as a barrier material in GaAs based heterostructure devices like in quantum well infrared photodetector (QWIP)[22]. And known about AlGaAs dust it is an irritant to skin, eyes and lungs [23].

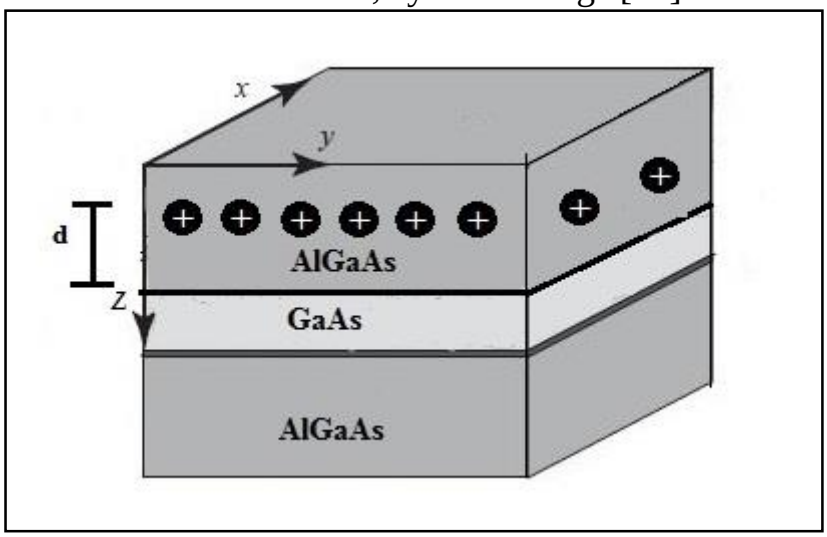

Figure (1.2): The structure of two-dimensional electron confined in GaAs layer bounded to an off donor impurity located in the AlGaAs layer.

1.3 Literature survey

Heterostructure material properties affected by several terms: the magnetic field, electrical field and the presence of donor impurity position, the most important and affected quantity is the energy. The donor impurity affects the Hamiltonian by adding a coulomb term which can be solved by several methods. Analytical, numerical, perturbation, variation, and diagonalization method were used to solve donor impurity problem. The donor binding energy had been studied for the QW by using variational method. The ground binding energy of the QW had been computed as a function of the donor impurity position and the QW width under different electric field strengths [9, 24]. In Ref [20, 25] the donor impurity energy spectrum had been studied for two dimensional heterostructure. In Ref. [20], the donor

impurity energy for the ground and excited state had been computed as a function of magnetic field strength, for both weak and strong magnetic field, using exact and perturbation methods [25].

Chuu *et al* in [26] obtained the donor impurity energy levels analytically for both donor impurity located at the quantum dots center, and for donor impurity located at the axis of the quantum-well wire. Zhu and Gu in Ref. [27] investigated the energy transition on shallow donor impurity states in a harmonic QD by using analytical method with the presence of the magnetic field. The energy transition change with the magnetic field strength, where the result show the high effects of magnetic fields on donor impurity energy states transition [27]. The dependence of the diamagnetic susceptibility and the binding energy of the donor impurity on the pressure and the temperature had been shown analytically. Khordad and Fathizadeh in Ref. [28] found in their recent study the diamagnetic susceptibility increases by increasing the pressure and it decreases with increasing the temperature. Peter in Ref. [29] the binding energy levels of shallow hydrogenic impurities are reported in a parabolic QD with pressure effect using variational approach. Where they found that the ionization energy is purely pressure dependence. Also Merchancano *et al* Ref. [30] had calculated the binding energy of hydrogenic impurities in a spherical QD using the variational and perturbation approaches as a function of pressure, QD size, and the impurity position. They found that the binding energy increases with increasing the pressure [30]. The combined effects of pressure and temperature on the binding energy of donor impurity in

a spherical QD with the presence of the electric field or without had been investigated [12, 31].

The problem of two electrons QD had been solved using exact diagonalization method with including the pressure and temperature effects. The magnetization and magnetic susceptibility of confined electrons in parabolic quantum dot was considered in experimental studies and theoretical calculations [32, 33].

Very recent, Elsaid *et al* in Ref. [34-42].has studied the electronic, thermodynamic and magnetic properties of two electrons confined in a single quantum dot and coupled quantum dots (CQD).

Alfonso *et al* in [43] had studied the energy states of an electron confined in a two dimensional (2D) plane and bound to an off-plane shallow donor center in the presences of an external magnetic field by using variatonal and numerical approach.

In this work, we will investigate the combined effects of pressure, temperature, magnetic field strength and the impurity position on the ground state binding energy of the donor impurity in heterostructure materials. In this study, we have computed the ground state energy level of donor impurity in a heterostructure by solving the donor impurity Hamiltonian using exact diagonalization method. In addition, we have study the effect of magnetic field strength, the confining frequency, pressure, and temperature on the binding energy.

1.4 Research objectives

There are two main aims of this research that can be summarized as follows:

1. To obtain the ground state energy of this system by solving the Hamiltonian using the exact numerical diagonalization method and compare the results with the **1/N** expansion [45]. The ground state energy will be calculated at specific values of the impurity distance (d) and the magnetic field strength.
2. To investigate the effect of pressure P and temperature T on the impurity ground state binding energy as a function of the magnetic field strength (γ and ω_c), impurity position (d), P and T.

1.5 Outlines of thesis

In this work, the ground state energy of GaAs/AlGaAs quantum heterostructure has been calculated as a function of the magnetic field strength with varying the impurity position and the confining frequency using the exact diagonalization method to solve the systems hamiltonian . Secondly, the effect of the pressure and temperature on the computed energy spectra of the quantum heterostructure will be found by using the effective mass approximation as a function of magnetic field strength, and the confining frequency. All numerical results are computed using Mathmatica Language Package.

The rest of this thesis is organized as follows: the Hamiltonian theory of donor impurity, the exact diagonalization technique and the parameters like

effective mass and dielectric constant on the pressure and temperature are presented in chapter II. In chapter III, the computed results of the donor impurity energy and the effects of the temperature and pressure had been displayed and discussed. The final chapter devoted for conclusions and future work.

Chapter two

Theory of donor impurity confined in heterostructure

This chapter mainly describes three important parts of the donor impurity formulation: The quantum heterostructure Hamiltonian, the exact diagonalization method and the pressure and temperature effects on the computed donor impurity ground state binding energy by the effective-mass approximation.

2.1 The Hamiltonian of donor impurity in a heterostructure in the presence of the magnetic field

The system is a quantum heterostructure in the x-y plane with the impurity in the z axis at the distance d, in the presence of a uniform external magnetic field strength B applied along the z direction.

The interaction between the electron in the GaAs layer and the impurity located in AlGaAs barrier is purely coulomb interaction. The Hamiltonian for this system is solved and discussed in appendix A.

The Hamiltonian operator for this model can be written as:

$$\widehat{H} = -\left(\rho^{-1/2}\frac{\partial^2}{\partial\rho^2}\rho^{1/2} + \frac{1}{\rho^2}\left(\frac{\partial^2}{\partial\phi^2} + \frac{1}{4}\right)\right) + \frac{1}{4}\omega^2\rho^2 - i\gamma\frac{\partial}{\partial\phi} - \frac{2}{\left|\rho - \vec{d}\right|} \quad (2.1)$$

This Hamiltonian in Eq. 2.1 can be separated into two parts as:

$$\hat{H} = \hat{H}_{\perp} + V(\rho) \quad (2.2)$$

where:

$$\hat{H}_{\perp} = -\left(\rho^{-1/2}\frac{\partial^2}{\partial\rho^2}\rho^{1/2} + \frac{1}{\rho^2}\left(\frac{\partial^2}{\partial\phi^2} + \frac{1}{4}\right)\right) + \frac{1}{4}\omega^2\rho^2 - i\gamma\frac{\partial}{\partial\phi} \qquad (2.3)$$

and

$$V(\rho) = -\frac{2}{|\rho - d|} = -\frac{2}{\sqrt{\rho^2 + d^2}} \qquad (2.4)$$

The potential $V(\rho)$ represents the Coulomb term. The Hamiltonian $\hat{H}_{\perp}$is a harmonic oscillator type with well known solution as shown later in eq.2.7 [19]. The complete details of donor Hamiltonian is shown in appendix A. In general, there is no analytical solution available for the complete donor impurity Hamiltonian.

2.2 Exact diagonalization method

In this thesis, we will use the exact diagonalization technique to solve the donor impurity Hamiltonian in problem given by Eq.(2.1) and study its electronic properties.

For zero donor impurity case $\hat{H}_{\perp}$, Eq.(2.1) reduces to harmonic oscillator type with a well known eigenstates |n,m> and eigenenergy. The basis (|n,m> $= \psi_{n,m}(\rho,\varphi)$) harmonic oscillator type wave function will be used to diagonalize the total Hamiltonian and obtain the ground state energy of the impurity system.

The basis wave functions are:

$$|\mathrm{n,m}> = \psi_{n,m}(\rho,\varphi) = \frac{1}{\sqrt{2\pi}}R_{n,m}(\rho)e^{im\varphi} \qquad (2.5)$$

where, $R_{n,m}(\rho)$=$e^{-\frac{1}{2}\rho^2\alpha^2}\rho^{|m|}\alpha^{|m|}\sqrt{\frac{2\alpha^2 n!}{(n+|m|)!}}\mathrm{L_n^{|m|}}(\rho^2\alpha^2)$ (2.6)

and eigenenergies

$$E_{n,m} = (2n + |m| + 1)\hbar\omega \tag{2.7}$$

where $L_n^{|m|}(\rho^2\alpha^2)$ is the standard associated Laguerre polynomials [19]. And α is an inverse length dimension constant which is given by:

$$\alpha = \sqrt{\frac{m\omega}{\hbar}} \tag{2.8}$$

These harmonic oscillator basis $|n, m>$ will be used to calculate the matrix elements of the full donor impurity Hamiltonian Eq.(2.1) $\langle R_{n,m}(\rho)|\hat{H}|R_{\acute{n},m}(\rho)\rangle$. We obtained the eigenenergies by using exact diagonalization method technique. Which explained in Appendix B.

In each calculation step the number of basis $|n, m>$ will be varied until a satisfy factor converging eigenenergies are achieved. The stability converging procedure is displayed in figures (3.1, 3.2, and 3.3).

The donor impurity binding energy (E_B) is defined as the difference between the energy states of the Hamiltonian (Eq. 2.1) without the presence of the impurity (E) and with its presence (E_0).

$$E_B = E - E_0 \tag{2.9}$$

2.3 The Pressure and Temperature effects on the impurity binding energy in a heterostructure.

The effects of the pressure (P) and the temperature (T) on the energy of the ground state can be investigated using effective mass approximation method (EMA). The pressure and temperature dependence of the material

electron effective mass, $m^*(P,T)$ and dielectric constant $\epsilon_r(P,T)$ are inserted in the impurity Hamiltonian as shown below

$$\hat{\mathrm{H}}(\rho) = \frac{1}{2m^*(P,T)}\left[\vec{p}(\rho) + \frac{e}{c}\vec{A}(\rho)\right]^2 + \frac{1}{2}m^*(P,T)\gamma^2\rho^2 - \frac{e^2}{\epsilon_r(P,T)\sqrt{\rho^2+d^2}} \qquad (2.10)$$

The mathematical dependences of $\epsilon_r(P,T)$ and $m^*(P,T)$ are given explicitly in appendix C.

Chapter three

Results and discussion

In this chapter we will show and discuss our computed results which are displayed in figures (from 3.1 to 3.19) and Tables 1-3 for heterostructure system made from GaAs. The material parameters are: dielectric constant $\epsilon = 12.4$, effective Rydber $R^* = 5.926\, meV$ and the effective mass of an electron $m^* = 0.067\, m_e$ ambient zero temperature and pressure. The impurity is located along z axis at the distance d, and with the presence of a uniform external magnetic field (B) along the z direction.

3.1 Binding energy of the donor impurity

In the first step of our present computational tasks, we have calculated the ground state eigenenergy (where m=0) for the donor impurity of GaAs/AlGaAs heterostructure as a function of the magnetic field strength γ with impurity located at the origin (d=0) for two specific values of the confinement frequency strength $\omega_0 = 5.412\, R^*$, and $\omega_0 = 3.044$ R*. The accuracy of our obtained results are tested against the corresponding ones produced by of $\frac{1}{N}$ expansion method [45]. The $\frac{1}{N}$ Expansion method is a powerful technique used to solve the spherical symmetric Hamiltonian function for any range of magnetic field strength as discussed in Ref [46,47]. Table 3.1 shows the comparison between the ground state (m=0) computed energy for the present exact diagonalization method and the

corresponding energy produced by $\frac{1}{N}$ expansion method. The comparison made in Table 3.1, shows a good agreement between both methods.

Table 3.1 : The ground state (m=0) energy (in R^*) by the computed energy for the exact diagonalization method against $\frac{1}{N}$ expansion method R3f.[45] for versus range of magnetic field strength .

		$\omega_0 = 5.412\ R^*$ Ground State Energy		$\omega_0 = 3.044\ R^*$ Ground State Energy	
γ	B(Tesla)	ExactMethod	$\frac{1}{N}$ Method	ExactMethod	$\frac{1}{N}$ Method
1	6.75	-2.11017	-2.15	-3.12522	-3.29
2	13.5	-2.05033	-2	-2.94692	-3.11
3	20.25	-1.74839	-1.76	-2.67781	-2.8
3.5	23.625	-1.60974	-1.61	-2.50864	-2.61
4	27.	-1.4569	-1.44	-2.32688	-2.39
4.5	30.375	-1.27918	-1.26	-2.11917	-2.26
5	33.75	-1.0966	-1.06	-1.90787	-1.92

To test the convergence issue of our exact diagonalization technique, we have plotted in figures 3.1, 3.2, and 3.3 the computed ground state energies (E) of the donor impurity Hamiltonian against the number of basis (n) from 1 to 38 for various value of confinement frequency ω_o , impurity distance d, and at magnetic field strength $\omega_c = 2\ R^*$. The figures clearly show the numerical stability in our computed scheme. The ground state approaches a limiting value as the number of basis increases. For example in Fig.3.2.a, the ground state energy approaches E= $-1.4\ R^*$ as we increase the number of basis up to 35.

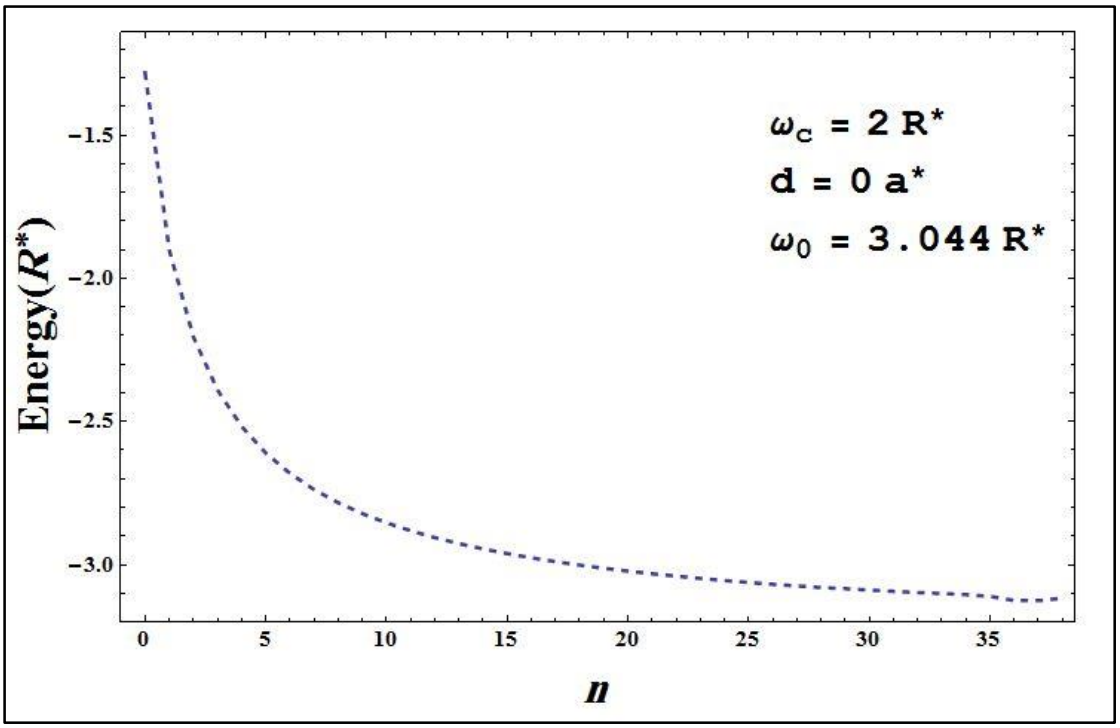

Fig. 3.1.a

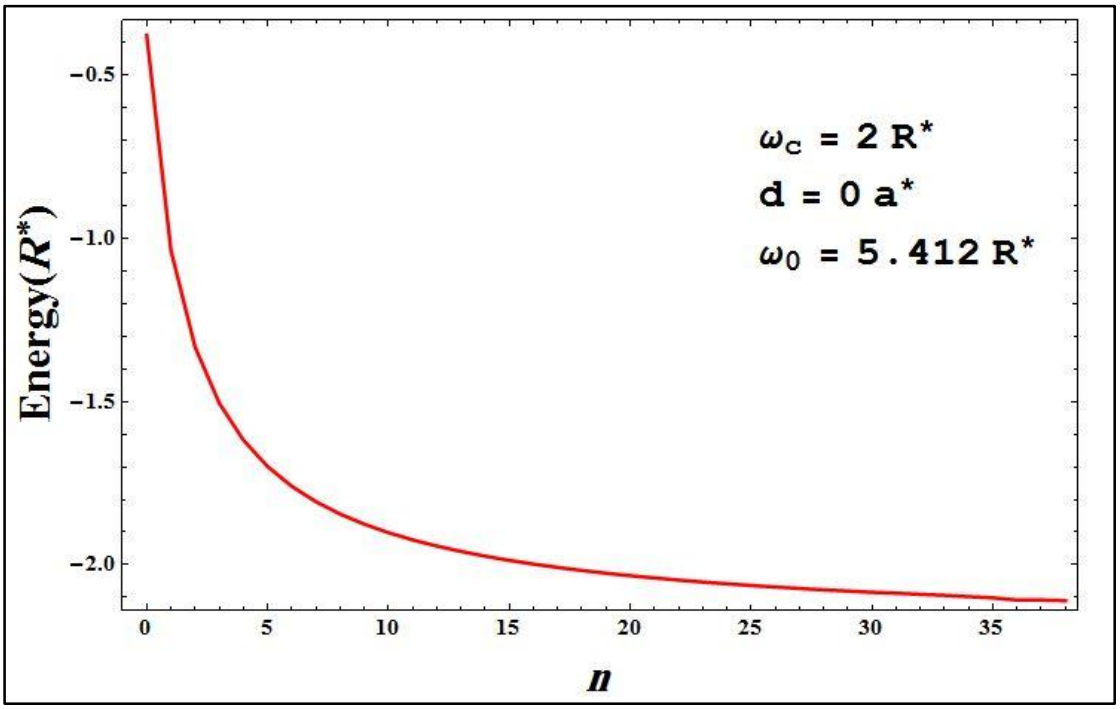

Fig. 3.1.b

Figure (3.1): The ground state energy of the quantum heterostructure for fixed value of $\boldsymbol{\omega_c = 2\,R^*}$ and at d = 0 $\boldsymbol{a^*}$ against the number of basis for: $\boldsymbol{a)\ \omega_0 = 3.044\ R^*}$ **and b)** $\boldsymbol{\omega_0 = 5.412\,R^*}$.

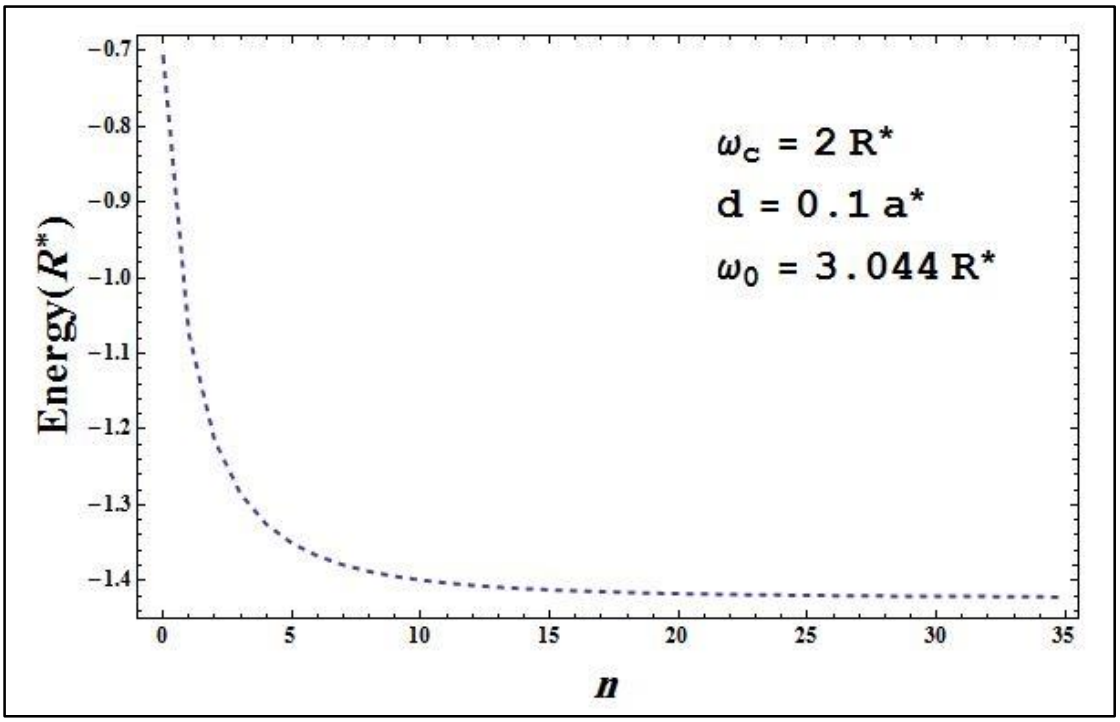

Fig. 3.2.a

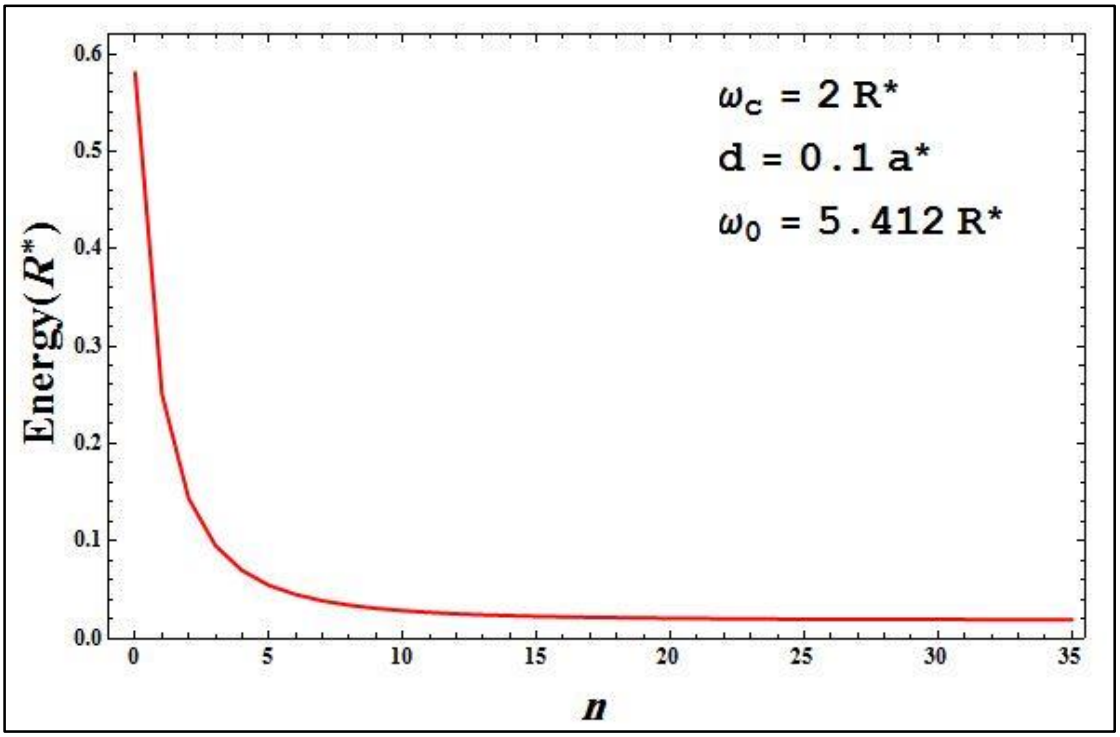

Fig. 3.2.b

Figure (3.2): The ground state energy of the quantum heterostructure for fixed value of $\boldsymbol{\omega_c = 2\,R^*}$ and at d = 0.1 $\boldsymbol{a^*}$ against the number of basis for: $\boldsymbol{a)\ \omega_0 = 3.044\ R^*}$ **and b)** $\boldsymbol{\omega_0 = 5.412\ R^*}$.

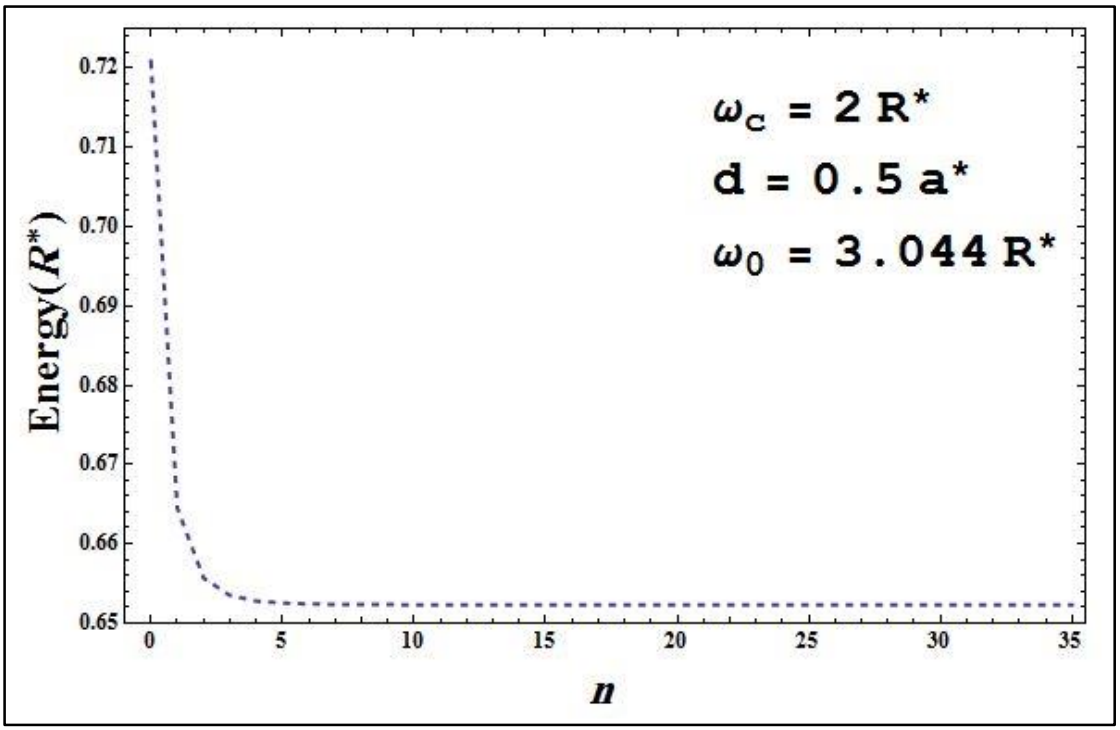

Fig. 3.3.a

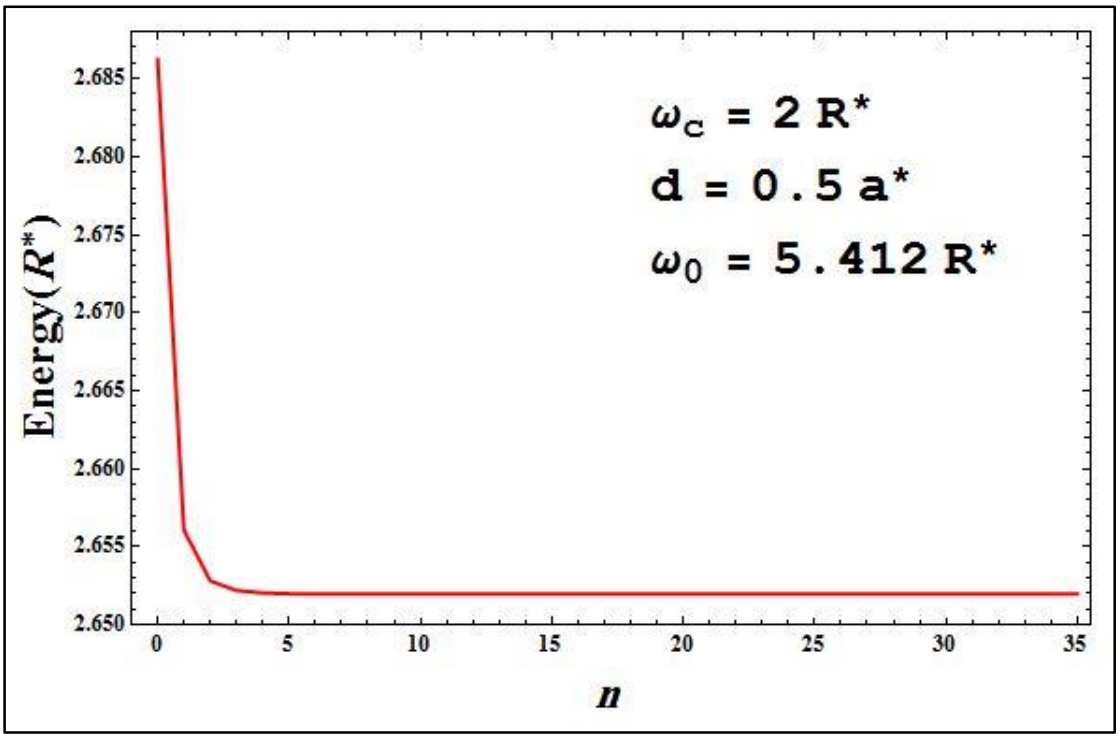

Fig. 3.3.b

Figure (3.3): The ground state energy of the quantum heterostructure for fixed value of $\boldsymbol{\omega_c = 2\,R^*}$ and at d = 0.5 $\boldsymbol{a^*}$ against the number of basis for: $\boldsymbol{a)\ \omega_0 = 3.044\ R^*}$ **and b)** $\boldsymbol{\omega_0 = 5.412\ R^*}$.

Figures 3.4 a and b display the energy of the donor impurity energy as a function of the magnetic field strength ω_c, for confinement frequencies $\omega_0 = 3.044R^*$ and $\omega_0 = 5.412R^*$, respectively. The solid line of the system indicates the absence of the impurity, and the dashed one indicates the presence of the impurity. It is clear from Fig. 3.4 that the effect of the impurity is decreasing the energy of the system. The presence of donor impurity lowers the energy of the heterostructure energy due to it negative coulomb attraction.

The energy of the heterostructure shows a significant dependence on the impurity position. Increasing the impurity distance (d) changing the system from 2D to 3D (bulk), and in this case the energy increases due to its great reduction in the attractive coulomb energy $(V(\rho) \sim -\frac{1}{\sqrt{\rho^2+d^2}})$, as displayed clearly in figure 3.5. For fixed values of impurity position (d), the energy of the donor Hamiltonian enhances as the confinement strength (ω_0) increases from 3.044 R^* to 5.412R^*. This energy behavior agrees with our expectation.

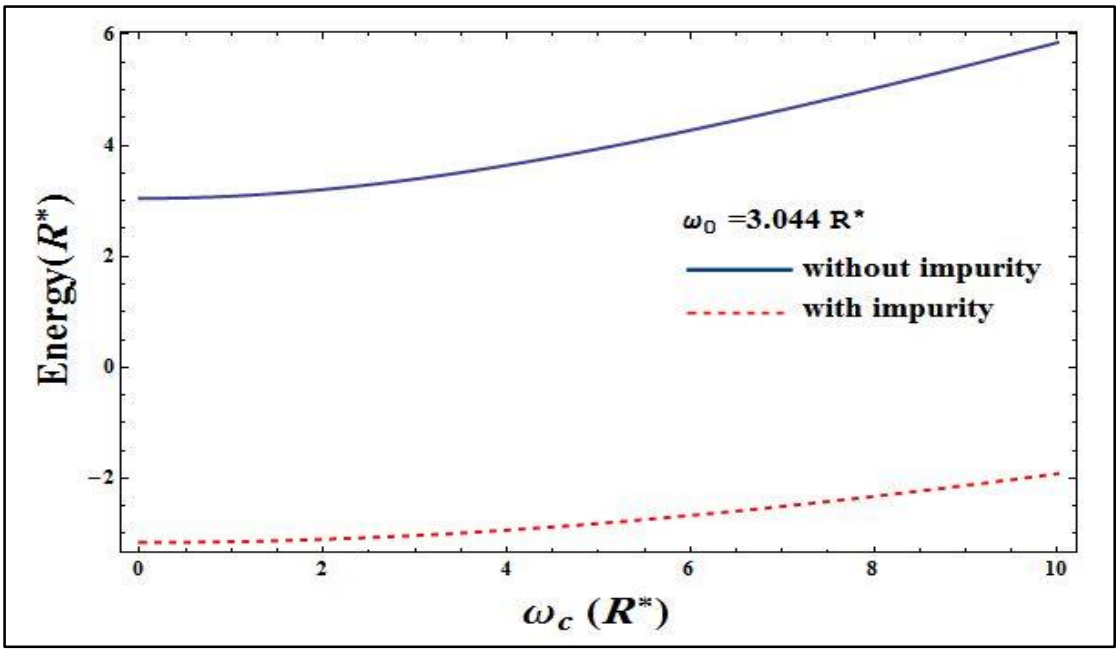

Fig. 3.4.a

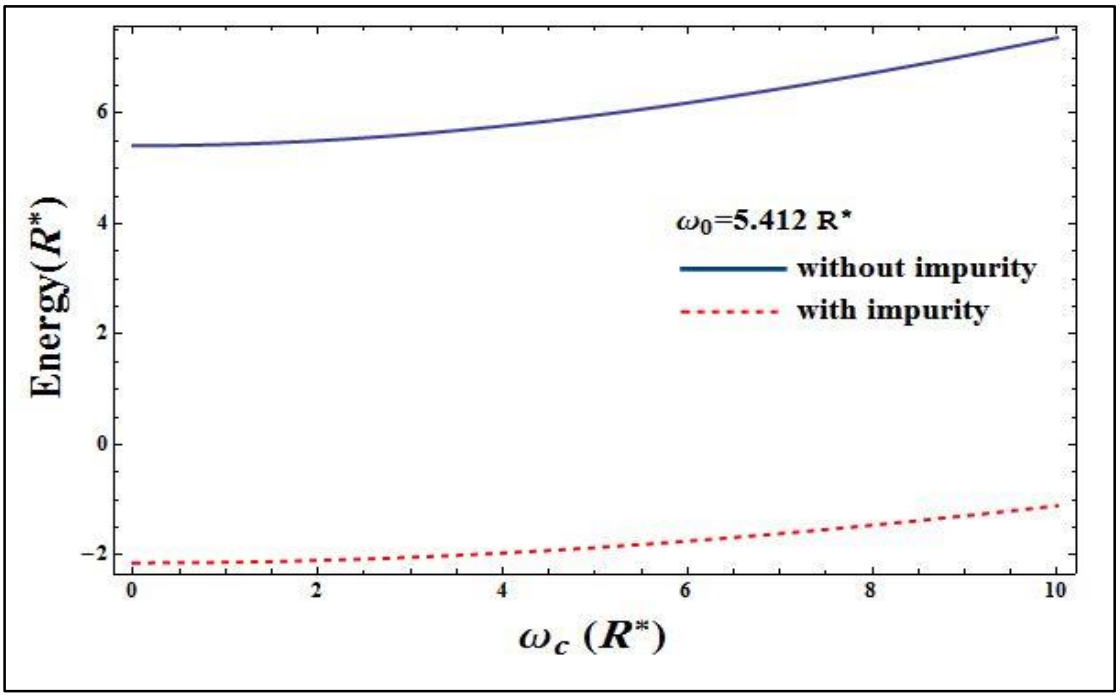

Fig. 3.4.b

Figure (3.4): The ground state energy of the quantum heterostructure for absence and presence of the impurity against the magnetic field strength $\boldsymbol{\omega_c}$ **the** dashed line with impurity and solid line for without impurity system **for**: **a**) $\boldsymbol{\omega_0 = 3.044\, R^*}$ and b) $\boldsymbol{\omega_0 = 5.412\, R^*}$.

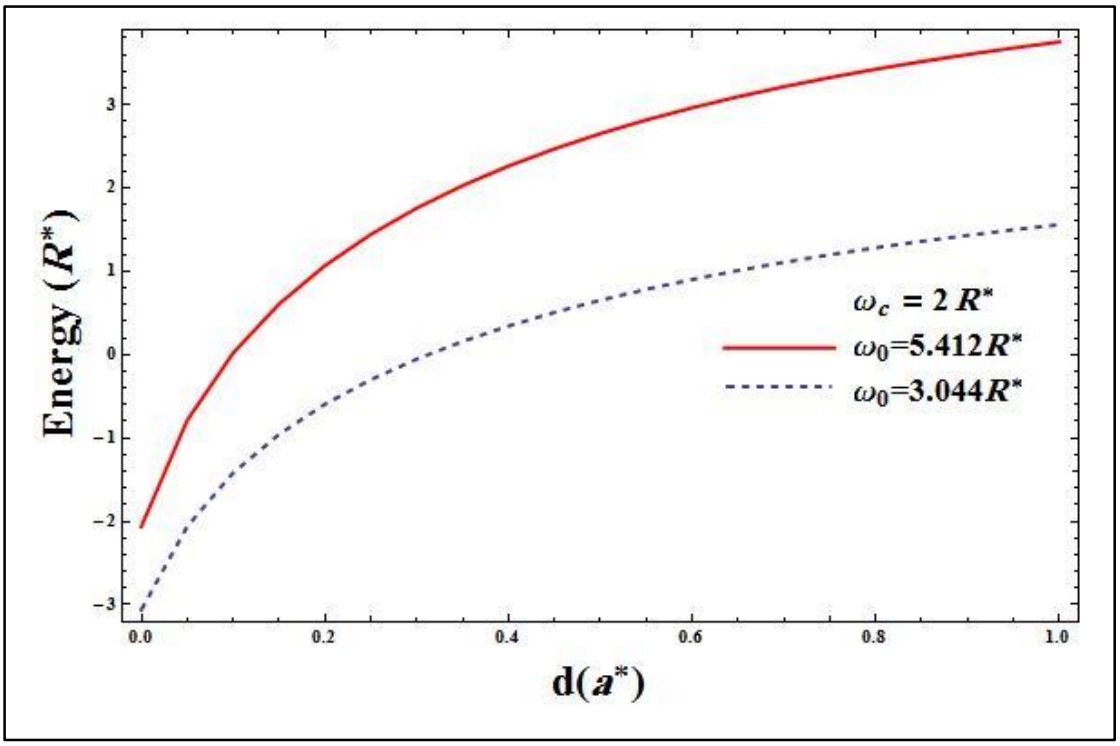

Figure (3.5): The ground-state for fixed value of $\boldsymbol{\omega_c = 2\,R^*}$against the distance for two $\boldsymbol{\omega_0}$, $\boldsymbol{\omega_0 = 3.044\,R^*}$**dashed line** ***and*** $\boldsymbol{\omega_0 = 5.412\,R^*}$ the solid line.

In the second computation step, we computed the ground-state eigenenergy (E) and the binding energy (E_B), for specific values of ω_0 and versus values of (d), against the magnetic field strength ω_c . In figure 3.6, we have presented the donor impurity ground state energy versus the magnetic field strength ω_c , for (a) d = 0 a^*, (b) d = 0.1 a^*, and (c) d = 0.5 a^*. It's clear from the three figures, and for particular fixed values of ω_0 and d that the energy increases as magnetic field strength ω_c increases. For fixed values of d and ω_c, the energy of donor impurity Hamiltonian increases as ω_0 increases.

For example at $\omega_c = 6\,R^*$ and d=0 a^*, the donor impurity energy E=$-2.6716033\,R^*$ for $\omega_0 = 3.044\,R^*$ while for $\omega_0 = 5.412\,R^*$ the energy is E=$-1.7453226\,R^*$.

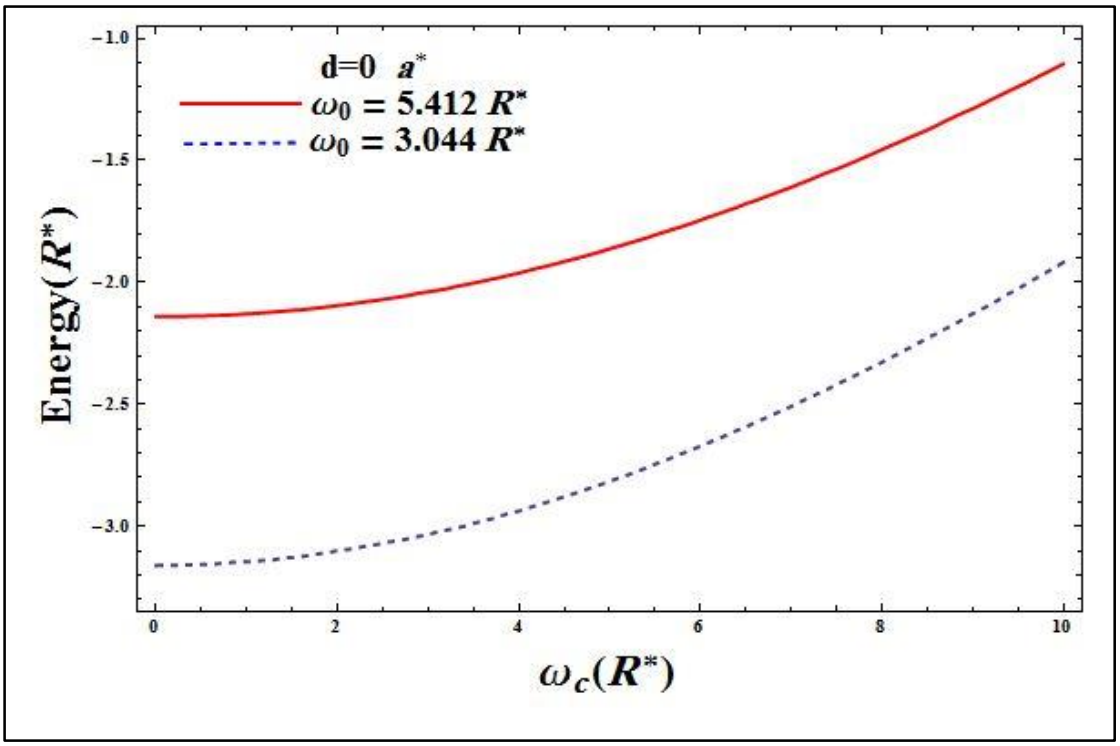

Fig. 3.6.a

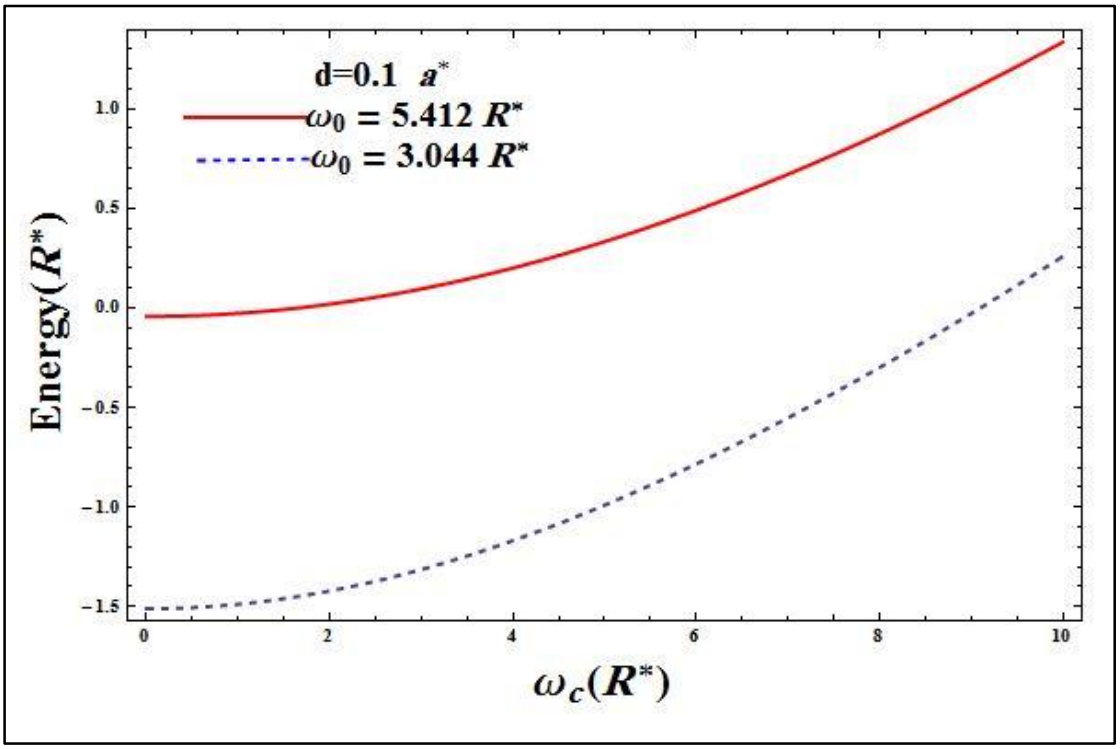

Fig. 3.6.b

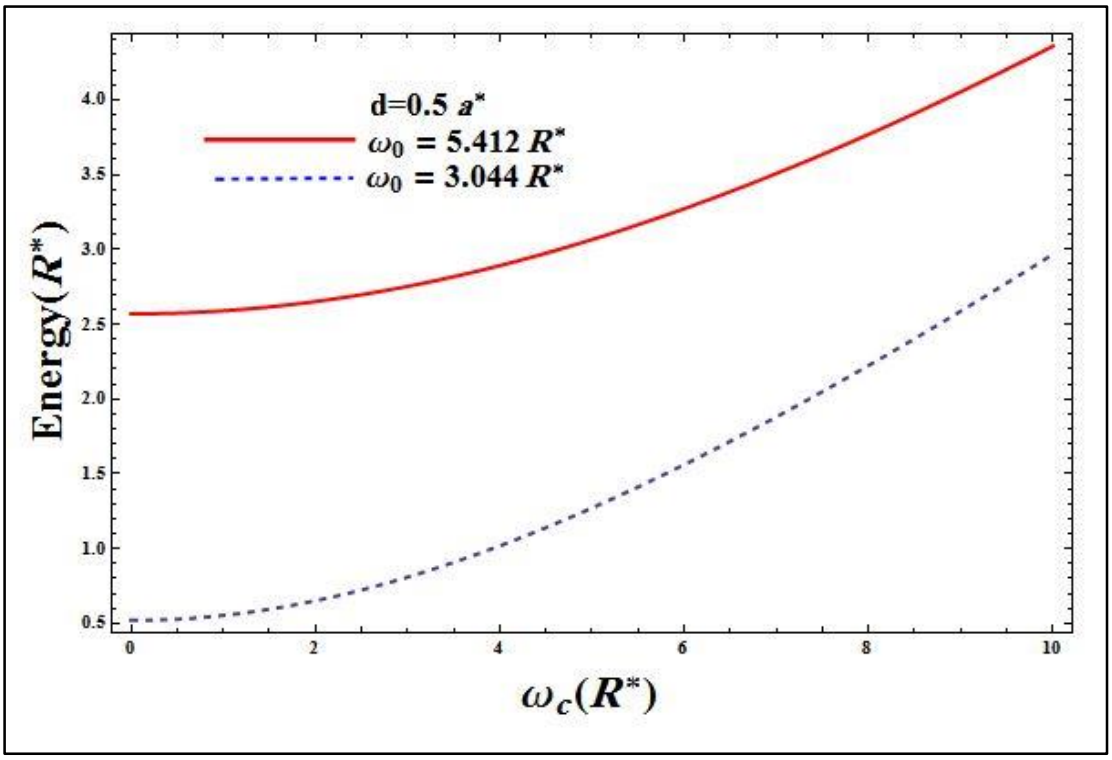

Fig. 3.6.c

Figure (3.6): The variation of the ground state energy with respect to the magnetic field strength ω_c , ω_0 , $\omega_0 = 3.044\ R^*$ **dashed line** $and\ \omega_0 = 5.412\ R^*$ the solid line, (a) for d=0 a^* , (b) d=0.1 a^*, and (c) d=0.5 a^*.

Figure 3.7 shows the dependence of the ground state binding energy (BE) on the magnetic field strength ω_c, for versus values of impurity distance d : (a) d=0 a^*, (b) d=0.1a^*, and (c) d=0.5a^* and confinement frequencies (ω_0 =3.044 R^* and ω_0 =5.412R^*). The binding energy E_B against the magnetic field strength for all distances (d), has the same behavior. The donor impurity binding energy almost shows the same qualitative behavior while its quantitative behavior changes as the impurity position (d) changes.

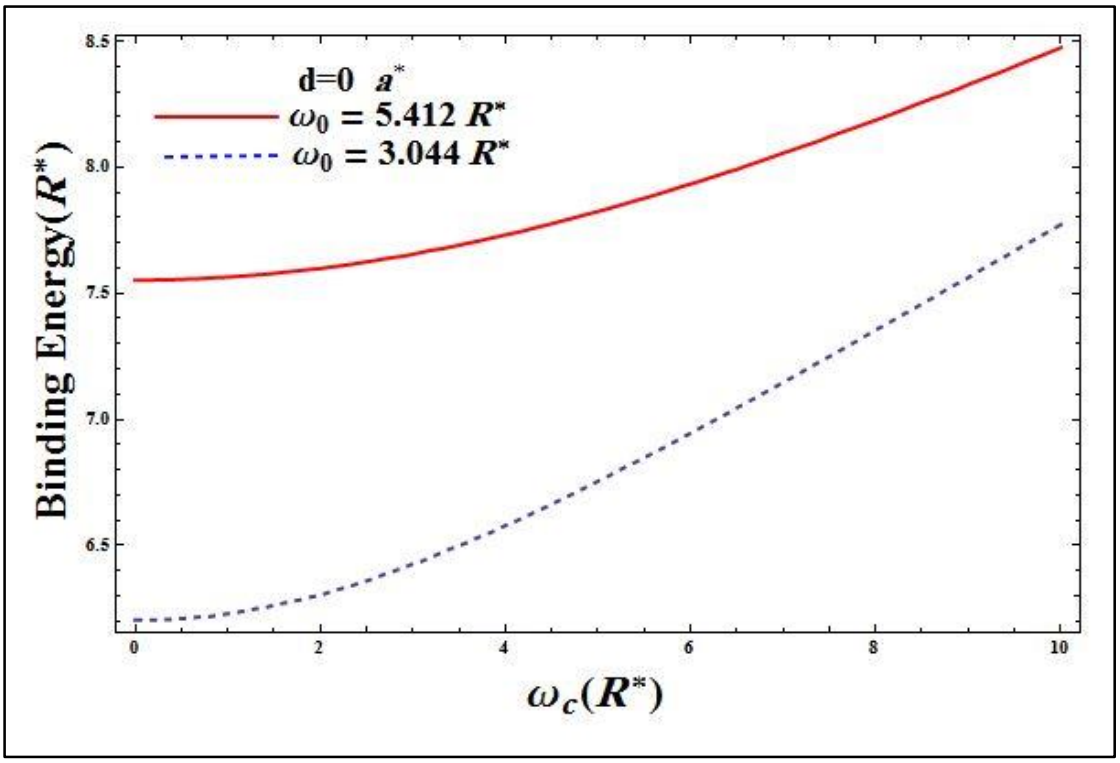

Fig 3.7.a

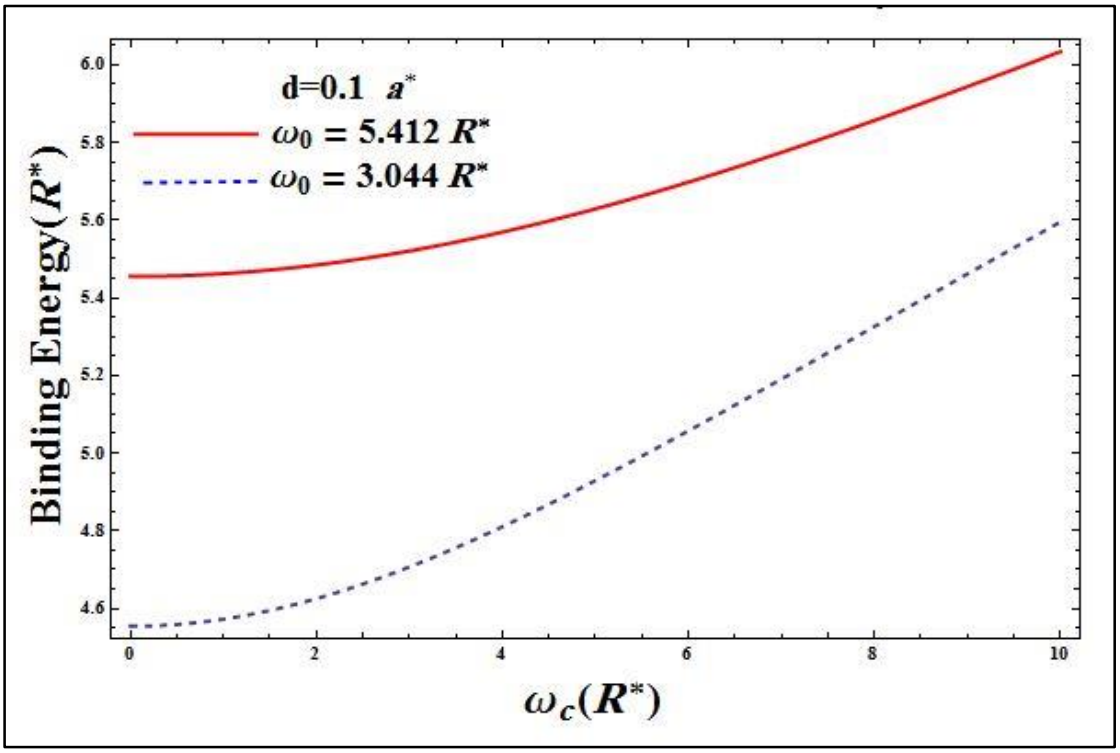

Fig 3.7.b

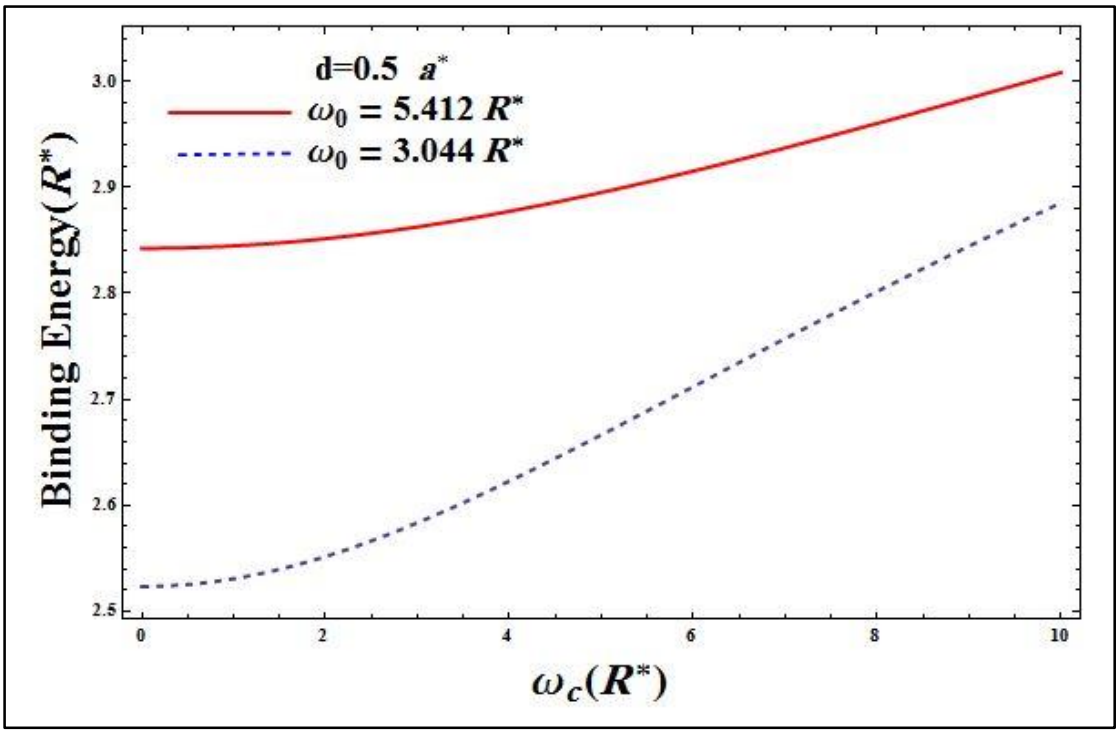

Fig 3.7.c

Figure 3.7: The ground-state binding energy against ω_c , where $\omega_0 = 3.044\ R^*$ **for dashed line**, **and** $\omega_0 = 5.412\ R^*$ **for solid line** (a) d = 0 a^* , (b) d = 0.1 a^*, and (c) d=0.5a^*.

Table 3.2 listed the donor impurity energy and binding energy as a function of magnetic field strength ω_c for $\omega_0 = 3.044\ R^*$ and for various values of d. For $\omega_0 = 3.044\ R^*$ and d=0 a^* , the binding energy increases as the magnetic field strength increases. This behavior persists for all d-values. However, the binding energy decreases as the impurity (d) increases. We can see a significant decrease in the binding energy as d increases from d=0.1 a^* to d=0.5 a^*. For example at $\omega_0 = 3.044\ R^*$ and $\omega_c = 2\ R^*$ the binding energy decreases significantly from 4.62499 R^* to 2.55177 R^*. This result is due to the great reduction in the coulomb impurity energy (Eq. 2.4), as we mentioned earlier. The same qualitative behavior can also be

observed in Table 3.3 with different quantitative behavior for $\omega_0 = 5.412\ R^*$.

Table 3.2: The donor impurity energy (E(R^*), and donor impurity binding energy ($E_B(R^*)$) against the magnetic field strength ω_c and various impurity position (d) for $\omega_0 = 3.044\ R^*$.

	d= 0 a^*		d=0.1 a^*		d=0.5 a^*	
wc(R^*)	E(R^*)	BE(R^*)	E(R^*)	BE(R^*)	E(R^*)	BE(R^*)
0.	-3.16072	6.20472	-1.50997	4.55397	0.520567	2.52343
0.5	-3.15595	6.21019	-1.50433	4.55858	0.528959	2.52529
1.	-3.14501	6.2298	-1.48746	4.57225	0.554005	2.53079
1.5	-3.12832	6.26336	-1.45957	4.5946	0.595315	2.53972
2.	-3.09887	6.30292	-1.42094	4.62499	0.652278	2.55177
2.5	-3.06943	6.36009	-1.372	4.66265	0.724104	2.56655
3.	-3.03356	6.42708	-1.31319	4.7067	0.809878	2.58364
3.5	-2.98742	6.4986	-1.24505	4.75624	0.90861	2.60258
4.	-2.93728	6.57952	-1.16812	4.81036	1.04276	2.62717
4.5	-2.87821	6.6635	-1.08295	4.86824	1.14089	2.6444
5.	-2.81585	6.75487	-0.990149	4.92918	1.27246	2.66656

Table 3.3: The donor impurity energy (E(R^*), and donor impurity binding energy ($E_B(R^*)$) against the magnetic field strength ω_c and various impurity position (d) for $\omega_0 = 5.412\ R^*$

	d= 0 a^*		d=0.1 a^*		d=0.5 a^*	
wc(R^*)	E(R^*)	BE(R^*)	E(R^*)	BE(R^*)	E(R^*)	BE(R^*)
0.	-2.14013	7.55213	-0.0426768	5.45468	2.56954	2.84246
0.5	-2.1377	7.55548	-0.0387892	5.45656	2.57473	2.84304
1.	-2.12914	7.56419	-0.0271437	5.46219	2.59026	2.84479
1.5	-2.11504	7.57876	-0.00779313	5.47151	2.61605	2.84767
2.	-2.09461	7.59822	0.0191767	5.48444	2.65196	2.85165
2.5	-2.07032	7.6248	0.0536489	5.50083	2.6978	2.85668
3.	-2.03883	7.65486	0.0954769	5.52055	2.75333	2.8627
3.5	-2.00289	7.69079	0.14449	5.54341	2.81827	2.86964
4.	-1.96213	7.73186	0.200496	5.56923	2.89231	2.87742
4.5	-1.91457	7.77565	0.263283	5.5978	2.97512	2.88596
5.	-1.86286	7.82438	0.332628	5.62889	3.06634	2.89518

3.2 Pressure and Temperature effects

In this section, we study the effects of the pressure and temperature on the ground-state binding energy of the donor impurity. We show in the Figures, from Fig.3.8 to Fig.3.19, the behavior of the donor binding energy (E_B) as a function of the magnetic field strength ω_c , impurity position (d), temperature (T), pressure (P) and confinement frequency ω_0. Figure 3.8 a shows the donor binding energy against the magnetic field strength for three different temperatures (5K, 100K, and 200K) and fixed values of pressure, impurity position d=0 a^* and confinement frequency $\omega_0 =$ 3.044 R^*. For fixed temperature, the figure clearly shows the enhancement of the binding energy as the magnetic field strength ω_c increases. This

enhancement in the donor binding energy can be attributed to the parabolic magnetic confinement term $\frac{1}{4}\omega^2\rho^2$ in eq.(2.3). For fixed values of magnetic field strength ω_c, the binding energy decreases when the temperature increases, as clearly shown in figure 3.8.a. Similar behavior of the donor binding energy is displayed in figure 3.8.b for different, $\omega_0 = 5.412\ R^*$.

In figure 3.9 we have show the dependence of the donor binding energy on the temperature for: fixed values of Pressure (P=10 Kbar), $\omega_c = 2\ R^*$, $d = 0\ a^*$ and various confinements ($\omega_0 = 3.044\ R^*$ and $\omega_0 = 5.412\ R^*$). The binding energy again shows a clear decreasing behavior as the temperature of the system increases. The dependence of the material parameter the effective mass m^*(P,T) and dielectric constant $\epsilon_r(P,T)$ on the temperature and pressure explain in Table C.1, where m^* decreases and ϵ_r increases with increasing T which diminish donor impurity binding energy E_B.

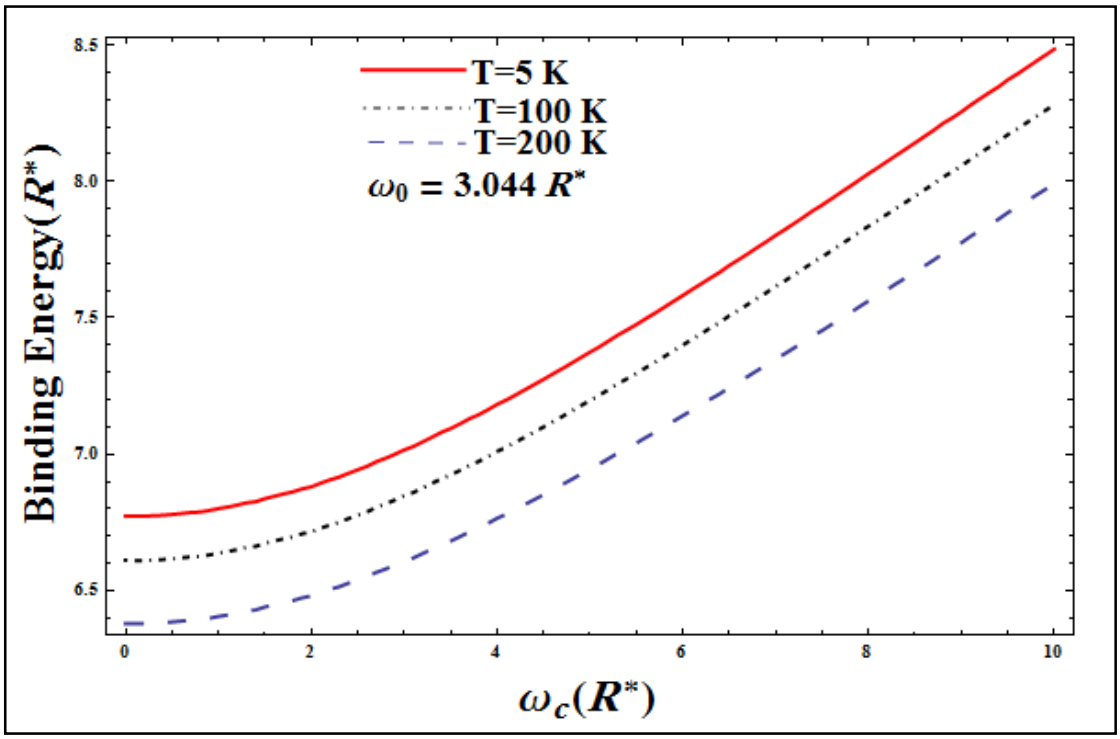

Fig. 3.8.a

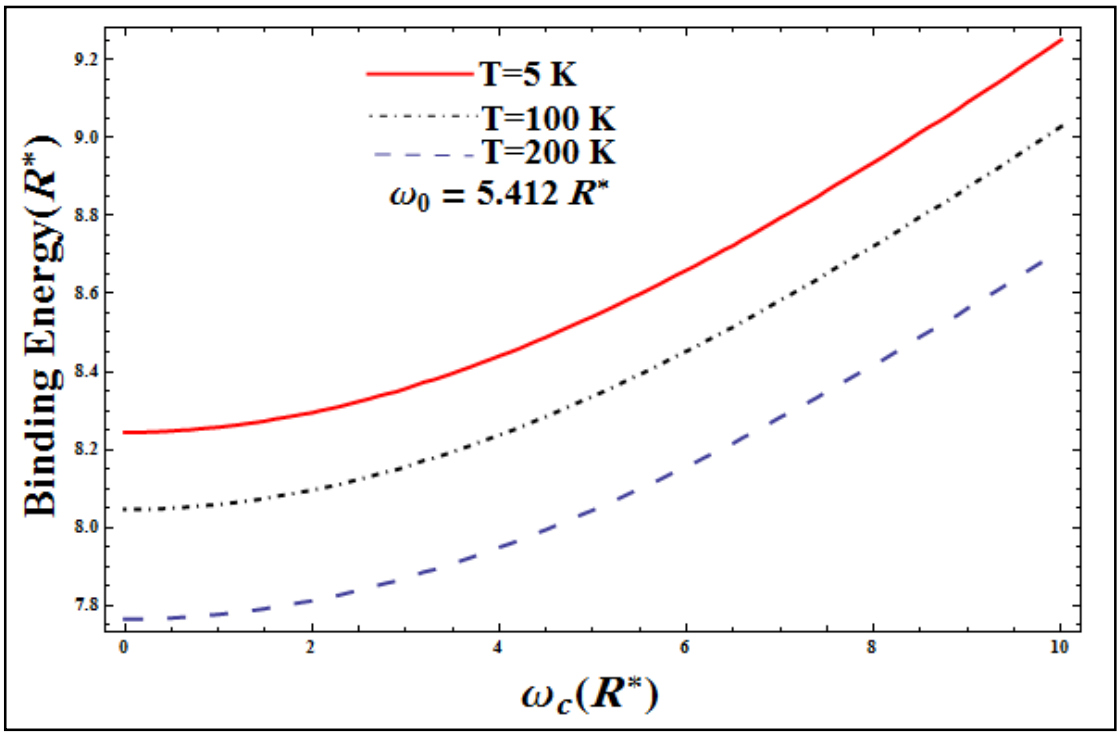

Fig. 3.8.b

Figure 3.8: The binding energy for d=0 $\boldsymbol{a^*}$ at constant Pressure (P=10 Kbar) as a function of $\boldsymbol{\omega_c}$ for 3 temperatures (5K, 100K, and 200K) for (**a**) $\boldsymbol{\omega_0 = 3.044\ R^*}$ **and b**) $\boldsymbol{\omega_0 = 5.412\ R^*}$.

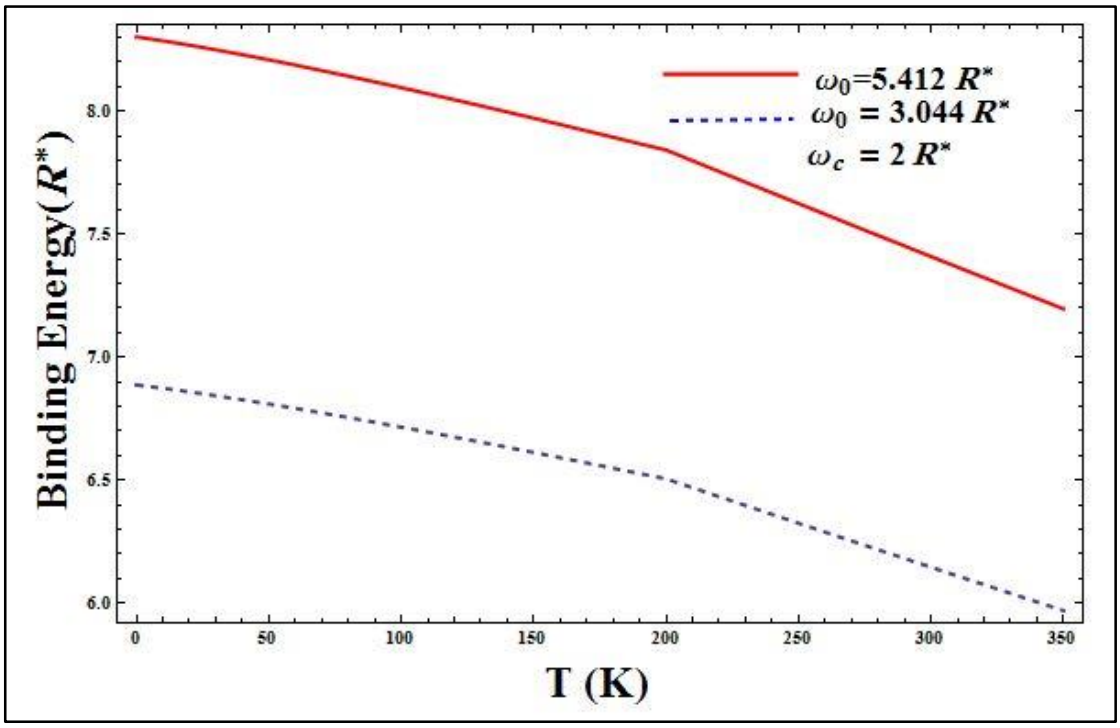

Figure 3.9 the binding energy change for d=0 $\boldsymbol{a^*}$ at constant Pressure (P=10 Kbar) and $\boldsymbol{\omega_c = 2\ R^*}$ with respect to the temperature **for $\boldsymbol{\omega_0 = 5.412\ R^*}$ solid line and for$\boldsymbol{\omega_0 = 3.044\ R^*}$ for the dashed line**

We show in figures 3.10 (a) and (b), the behavior of the donor binding energy as a function of the magnetic field strength ω_c , $\omega_0 = 5.412\ R^*$ and $\omega_0 = 3.044\ R^*$ for different values of pressure (0, 10, and 20) Kbar, impurity position d=0a^*, and temperature T=20 K. The donor binding energy shows a significant increase as the magnetic field ω_c increases, increasing ω_c decrease the electron-atom distance which increase the electron confinement. The binding energy again shows a great enhancement as the pressure increases, while keeping the magnetic field values unchanged.

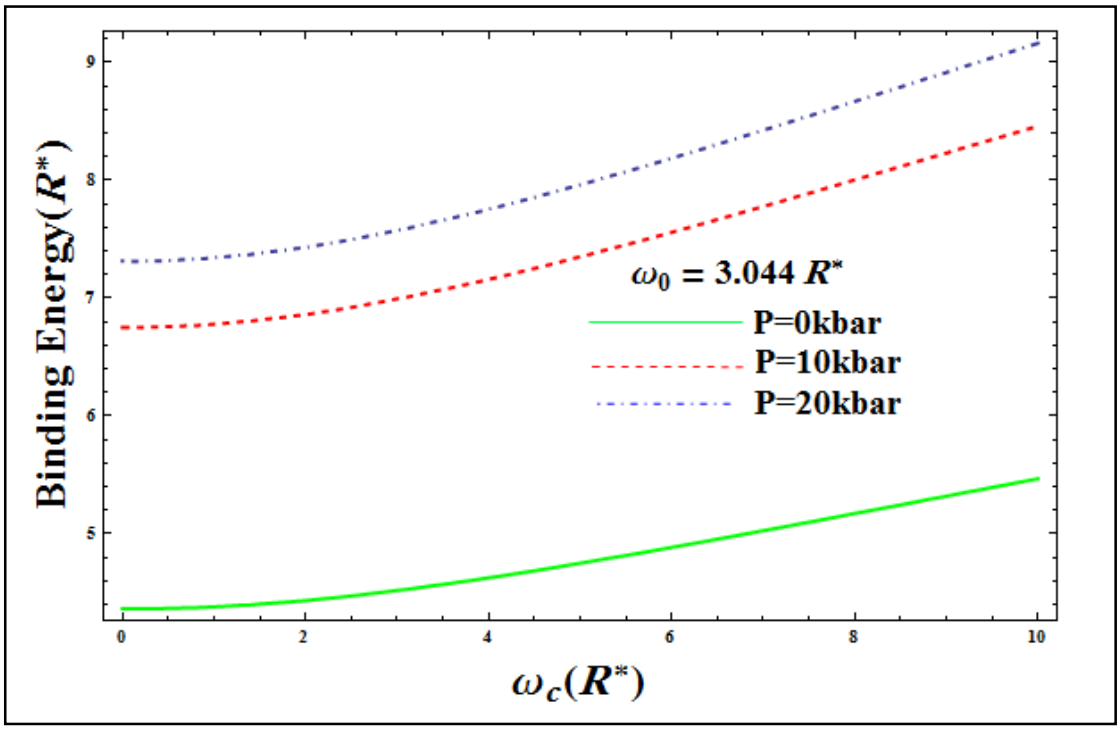

Fig.3.10.a

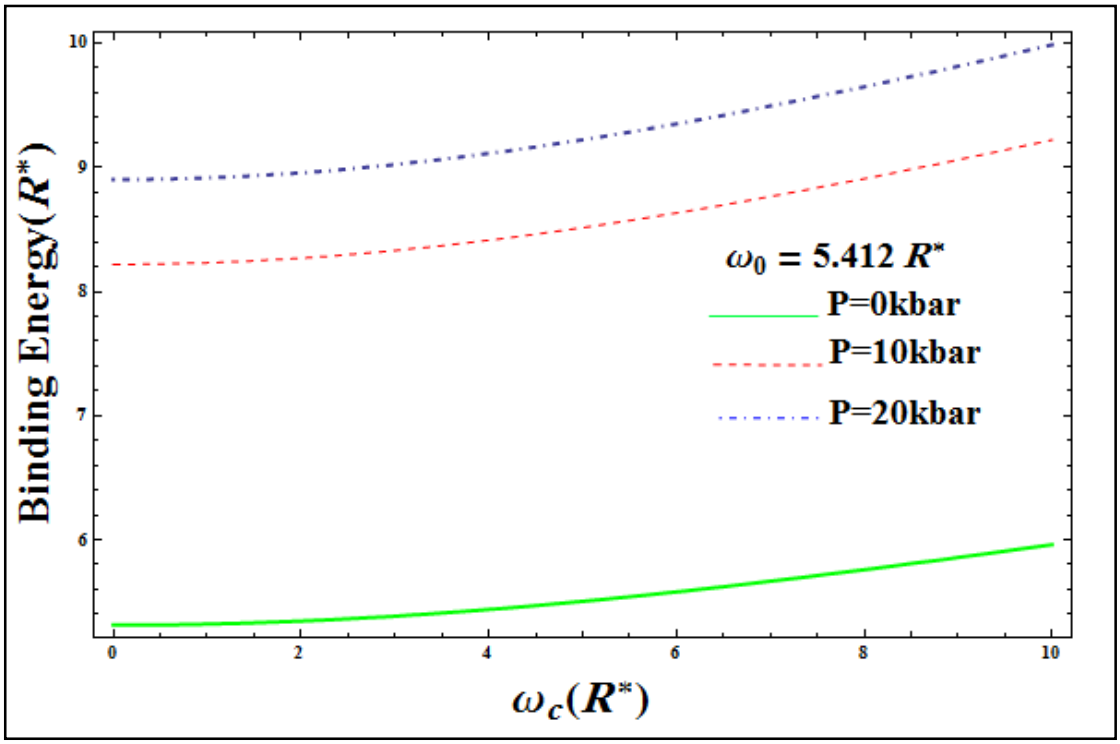

Fig.3.10.b

Figure 3.10: The variation of ground-state binding energy for d=0$\boldsymbol{a}^*$ against the $\boldsymbol{\omega_c}$ at fixed Temperature (20K) and for three different values of pressure (0, 10, and 20 Kbar) a) $\boldsymbol{\omega_0 = 3.044\ R^*}$ $\boldsymbol{b)}$ $\boldsymbol{\omega_0 = 5.412 R^*}$

In figure 3.11, we fixed the temperature (T=20K)

$\omega_c = 2R^*$ and $d = 0\ a^*$ parameters, while changing the pressure. We observe a great enhancement in the donor binding energy as the pressure increases for $\omega_0 = 3.044\ R^*$ and $\omega_0 = 5.412\ R^*$. This behavior because increasing the pressure increase m^* and decrease ϵ_r which enhance E_B.

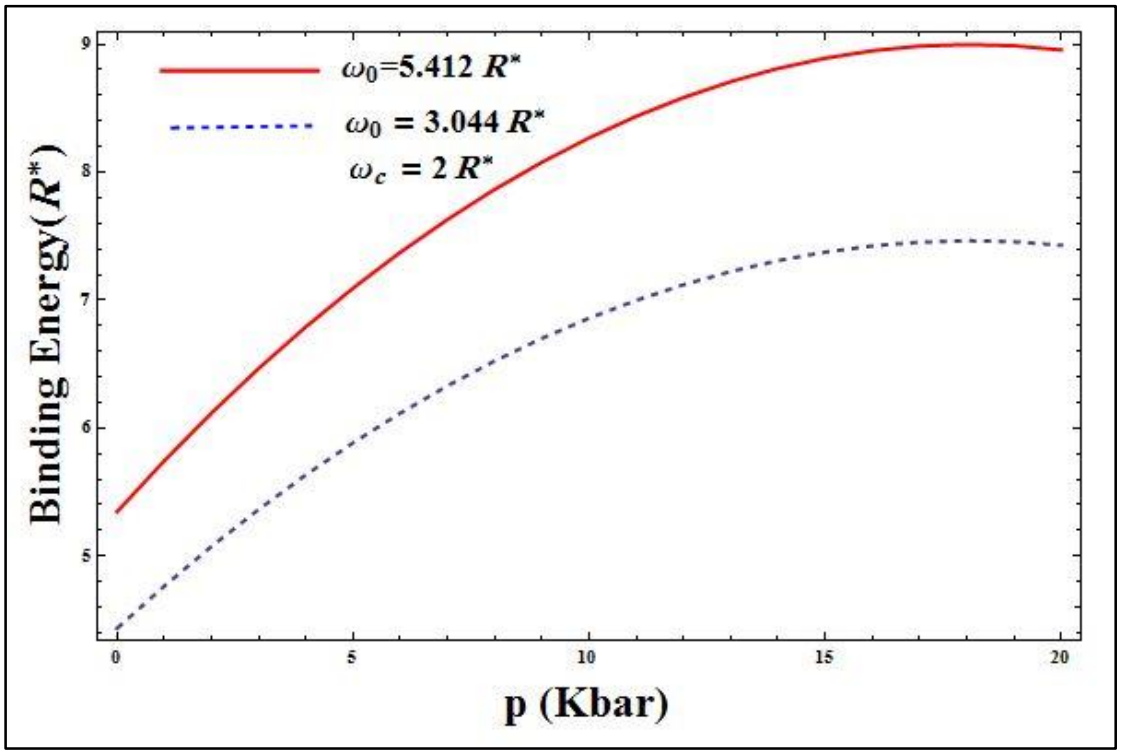

Figure 3.11: the variation of ground-state binding energy for d = 0 $\boldsymbol{a^*}$ against the pressure at fixed Temperature (20K) and $\boldsymbol{\omega_c = 2\ R^*}$ for $\boldsymbol{\omega_0 = 3.044\ R^*}$**and for** $\boldsymbol{\omega_0 = 5.412 R^*}$

In Figure 3.12 (a) and (b), we show the effect of changing the temperature at impurity position (d= 0.1 a^*) on the binding energy. Again, the binding energy shows great enhancement as we increase the magnetic field strength ω_c for fixed values of the parameters: Temperature (T= 5, 100, and 200K), Pressure (P=10 Kbar) and confinements frequency $\omega_0 =$ 3.044 $R^*$and $\omega_0 = 5.412$ R^*. We display in figure 3. 13 the donor binding energy against the temperature (T), while the rest of the physical parameters of the system are kept fixed. The binding energy shows an important dependence on the temperature, and the B.E decreases with increasing the temperature. The decreasing reason of E_B again comes from the effects of m^* and ϵ_r as mention on the explanation of figure 3.8 and 3.9.

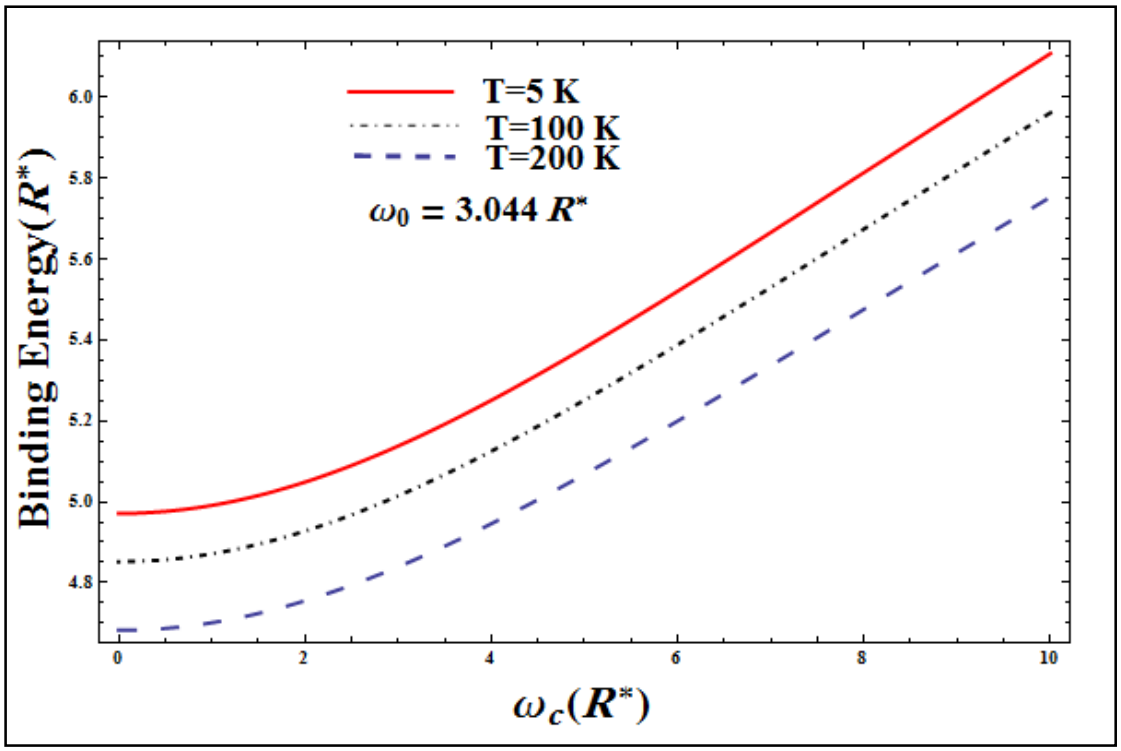

Fig. 3.12.a

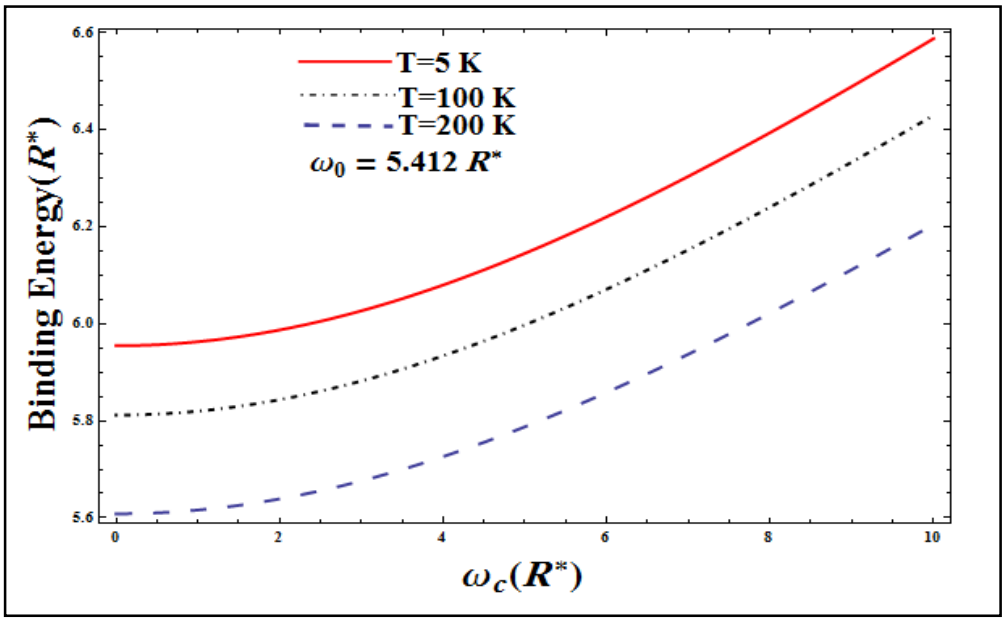

Fig. 3.12.b

Figure 3.12: The ground-state binding energy for d=0.1$\boldsymbol{a}^*$ at constant Pressure (P=10 Kbar) as a function of $\boldsymbol{\omega_c}$ and for three temperatures (5K, 100K, and 200K): **a**) $\boldsymbol{\omega_0 = 3.044\ R^*}$ **and b**) $\boldsymbol{\omega_0 = 5.412\ R^*}$.

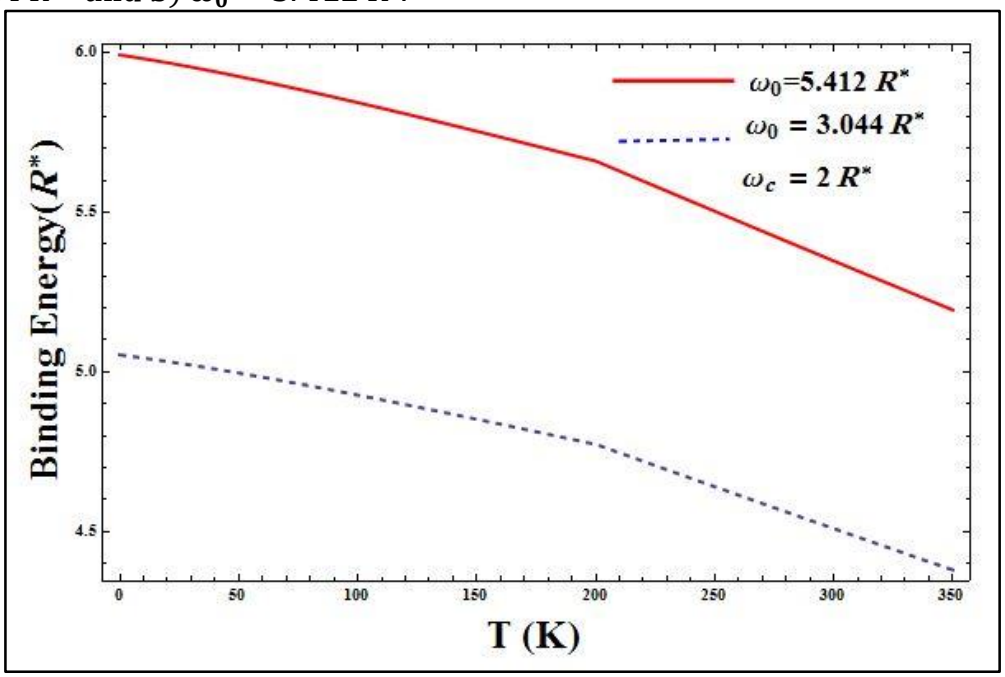

Figure 3.13: The ground-state binding energy for d = 0.1 $\boldsymbol{a}^*$ at constant pressure (P=10 Kbar) and $\boldsymbol{\omega_c = 2\ R^*}$, and temperature **for** $\boldsymbol{\omega_0 = 3.044\ R^*}$ **dashed line and for** $\boldsymbol{\omega_0 = 5.412\ R^*}$ **for the solid line**.

In figure 3.14 (a) and (b), we illustrate the pressure effect on the donor binding energy for d=0.1a^* against the magnetic field strength ω_c. Fig.3.14.a obviously shows that the binding energy increases as the magnetic field strength enhances while the pressure (0, 10, and 20 Kbar), T and d, and $\omega_0 = 3.044\ R^*$ are fixed. Fig.3.14.b shows the same behavior of the E_B but for different confinements $\omega_0 = 5.412\ R^*$. Effective-mass approximation investigate the pressure effects on m^* and ϵ_r, where it shown in Table C.1 which explain the reason of enhancing E_B.

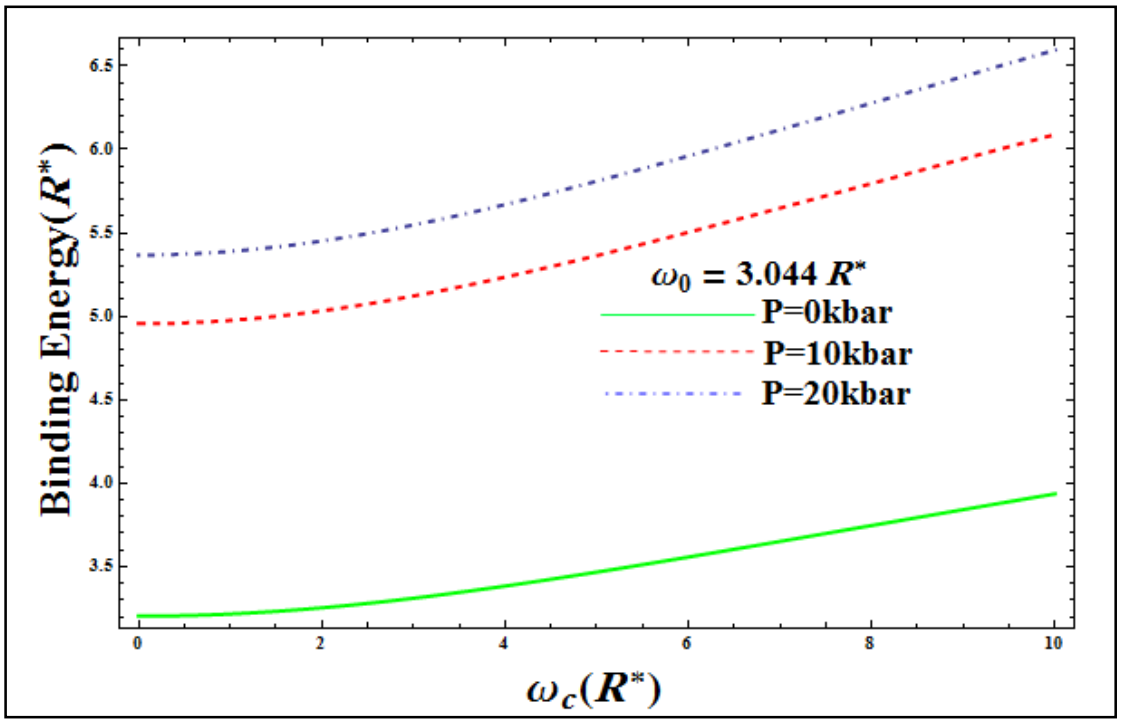

Fig. 3.14.a

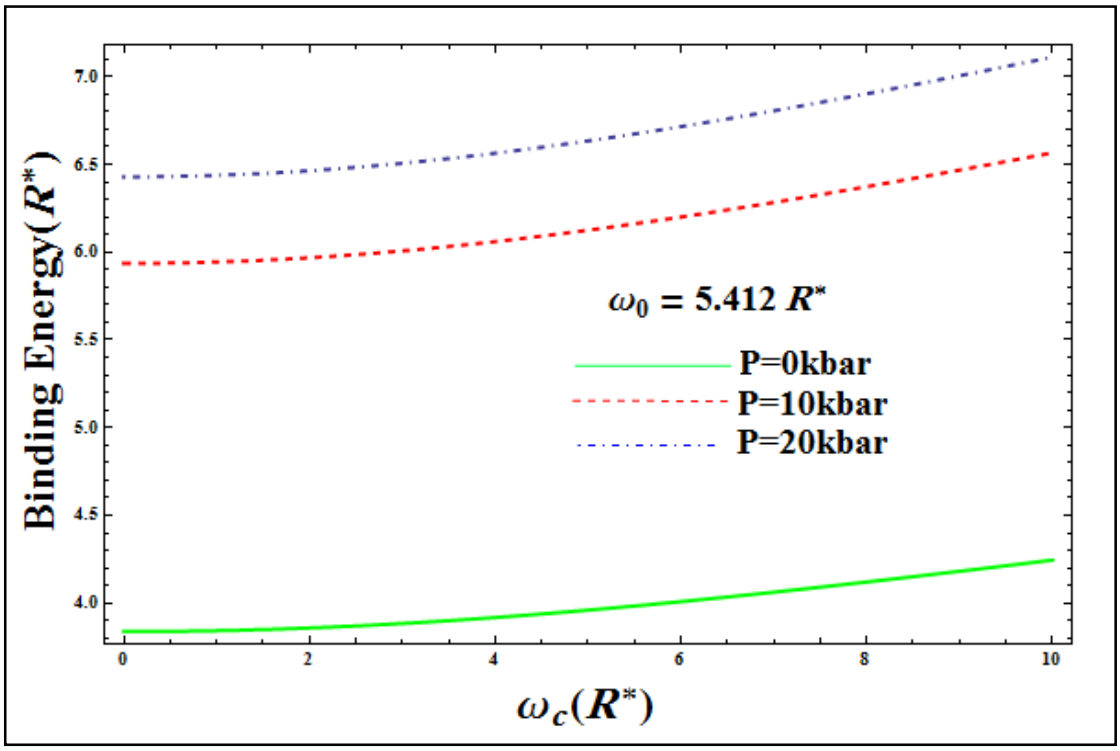

Fig. 3.14.b

Figure 3.14: the variation of binding energy for d=0.1$\boldsymbol{a^*}$ against the $\boldsymbol{\omega_c}$ at fixed Temperature (20K) for three pressure values (0, 10, and 20 Kbar) a) for $\boldsymbol{\omega_0 = 5.412\ R^* b)}$ **and for** $\boldsymbol{\omega_0 = 3.044\ R^*}$.

In Fig. 3.15, we plot the binding energy for the ground state as a function of the pressure for fixed values of T=20K, d $= 0.1\ a^*$, $\omega_c = 2R^*$, and at different confinements: $\omega_0 = 3.044R^*$ and $\omega_0 = 5.412\ R^*$. The E_B shows a great enhancement as the pressure increases for fixed values of confinement frequency because of increasing m^* and decreasing ϵ_r .

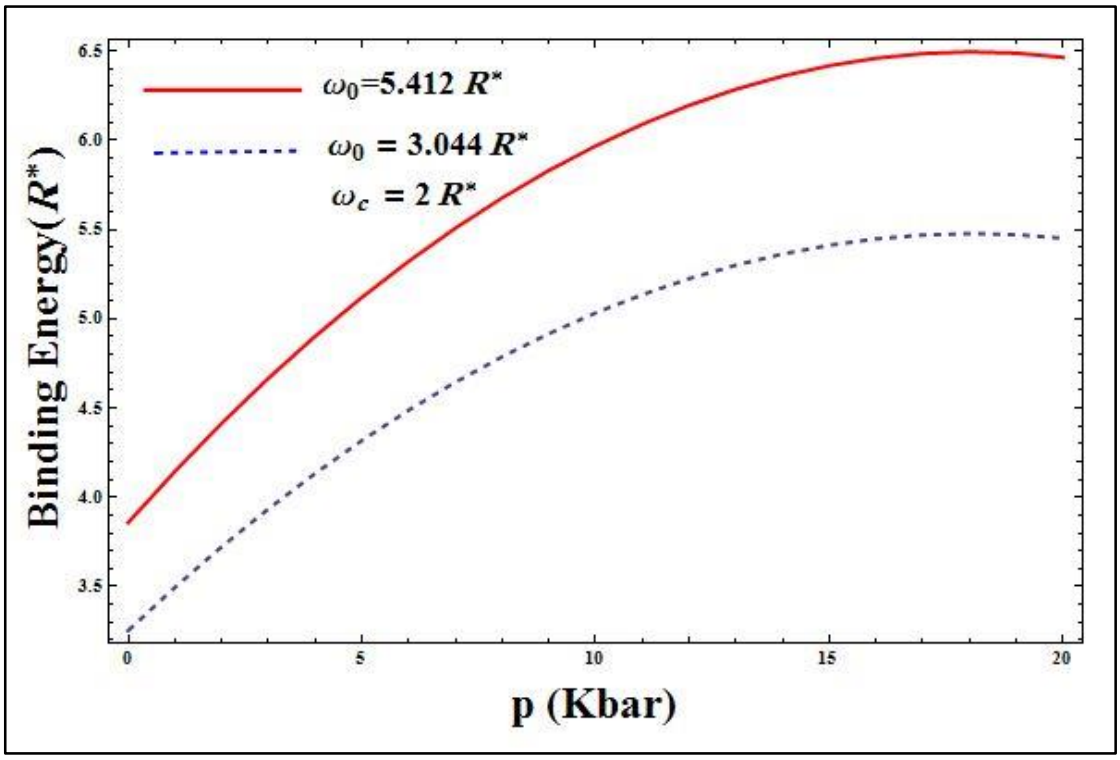

Figure 3.15: the variation of ground-state binding energy for d=0.1$\boldsymbol{a}^*$ as a function of the pressure at fixed Temperature (20K) and $\boldsymbol{\omega_c = 2\ R^*}$ for $\boldsymbol{\omega_0 = 3.044\ R^*}$ **and** $\boldsymbol{\omega_0 = 5.412\ R^*}$

Figure 3.16 (a) and (b), show the binding energy as a function of magnetic field strength but for d=0.5a^*. We have shown in figure 3.17 the dependence of the donor binding energy against the temperature for d=0.5a^* and various confinement frequencies $\omega_0 = 3.044\ R^*$ and $\omega_0 = 5.412\ R^*$and the rest parameter are fixed. The behavior is in agreement with the results explained in Fig. 3.9 (d=0a^*) but for d=0.5a^*.

The results presented in figure 3.18 (a) and (b) show the same qualitative behavior as given in figure 3.10 a and b (d=0 a^*). Fig. 3.18 shows the effect of pressure for (d=0.5a^*) on the E_B as a function of magnetic field strength. With make comparison between two d values (d=0 and 0.5 a^*) as we increase d, the binding energy increases due to the great reduction in the

coulomb attraction energy (eq. 2.4). In figure 3.19, we display the results of the donor binding energy for d=0.5a^*. The behavior agrees with the E_B behavior given in Fig.3.11 (for d=0 a^* with same reason).

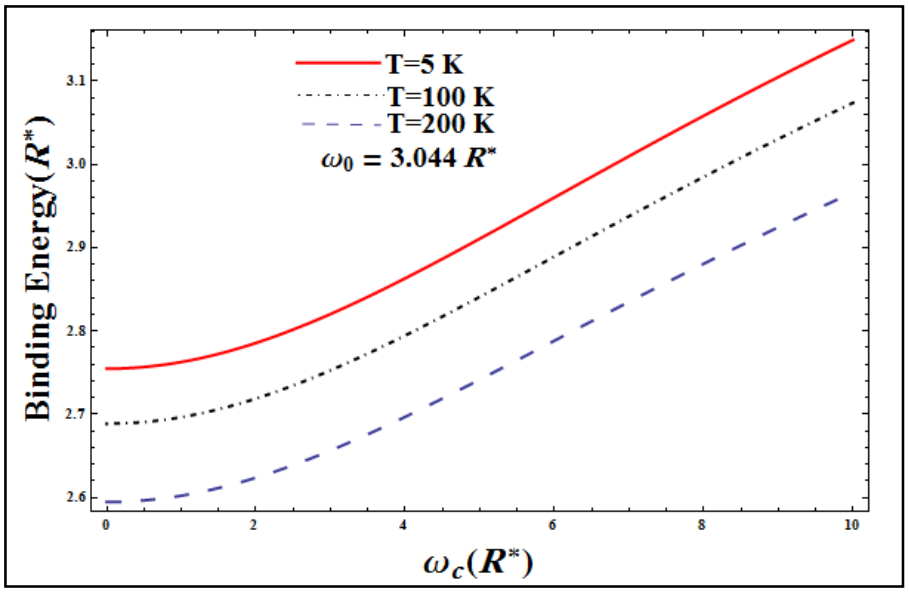

Fig. 3.16.a

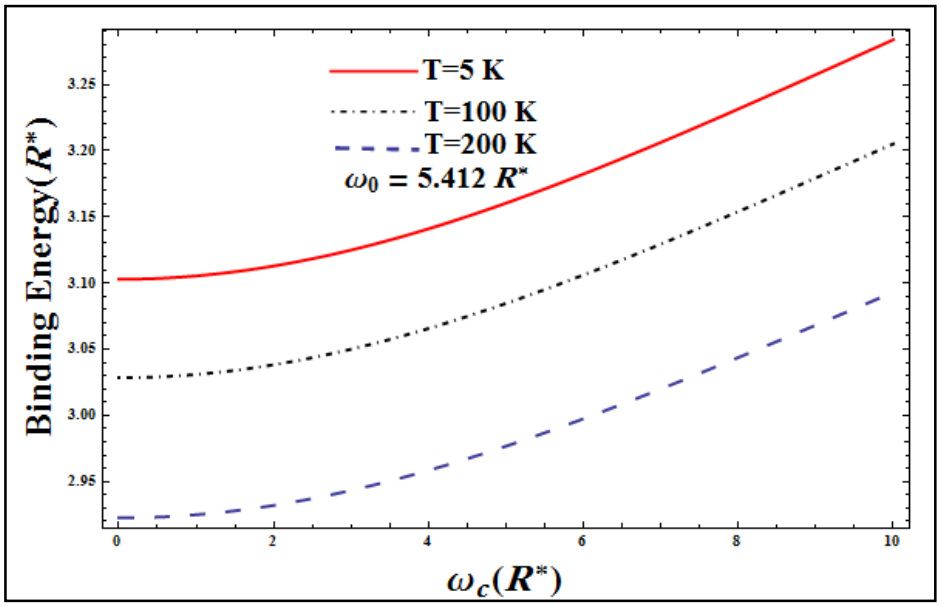

Fig.3.16.b

Figure 3.16: the binding energy for d=0.5$\boldsymbol{a}^*$ at constant Pressure (P=10 Kbar) as a function of $\boldsymbol{\omega_c}$ for 3 temperatures (5K, 100K, and 200K): **a)** $\boldsymbol{\omega_0 = 3.044\ R^*}$ **and b)** $\boldsymbol{\omega_0 = 5.412\ R^*}$.

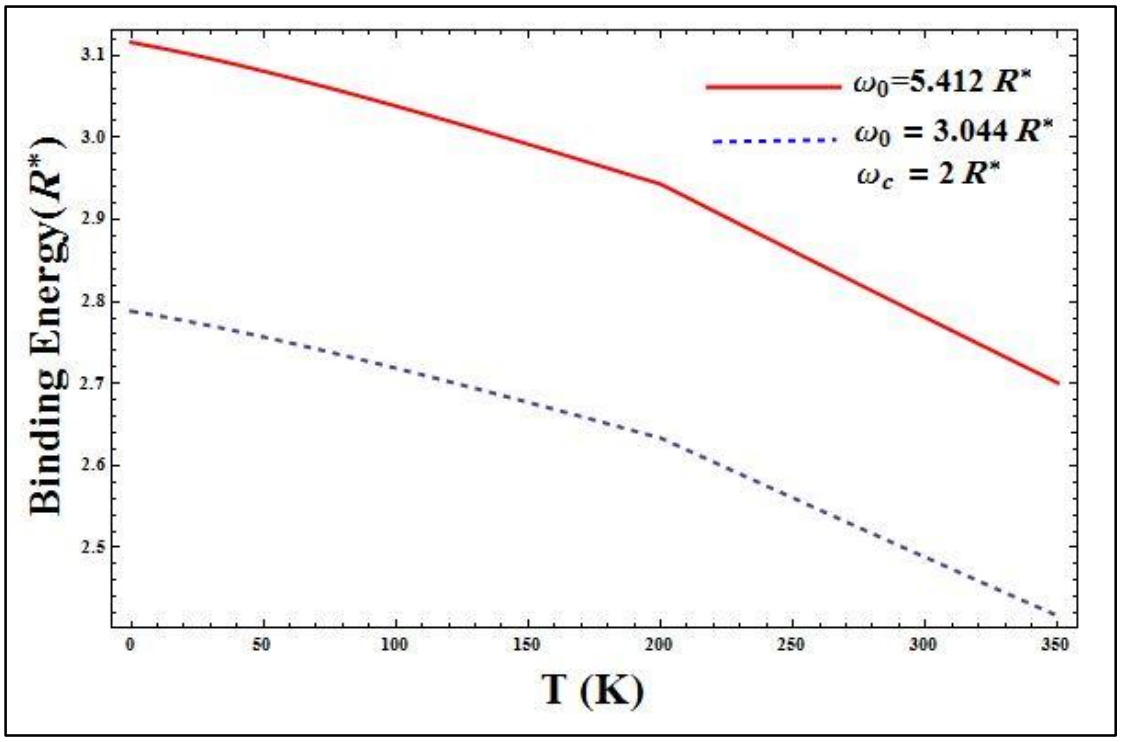

Figure 3.17: the binding energy for d=0.5 $\boldsymbol{a}^*$ at constant Pressure (P=10Kbar) and $\boldsymbol{\omega_c = 2\ R^*}$ against temperature **for $\boldsymbol{\omega_0 = 3.044\ R^*$ for the dashed line and for $\boldsymbol{\omega_0 = 5.412\ R^*$ solid line**.

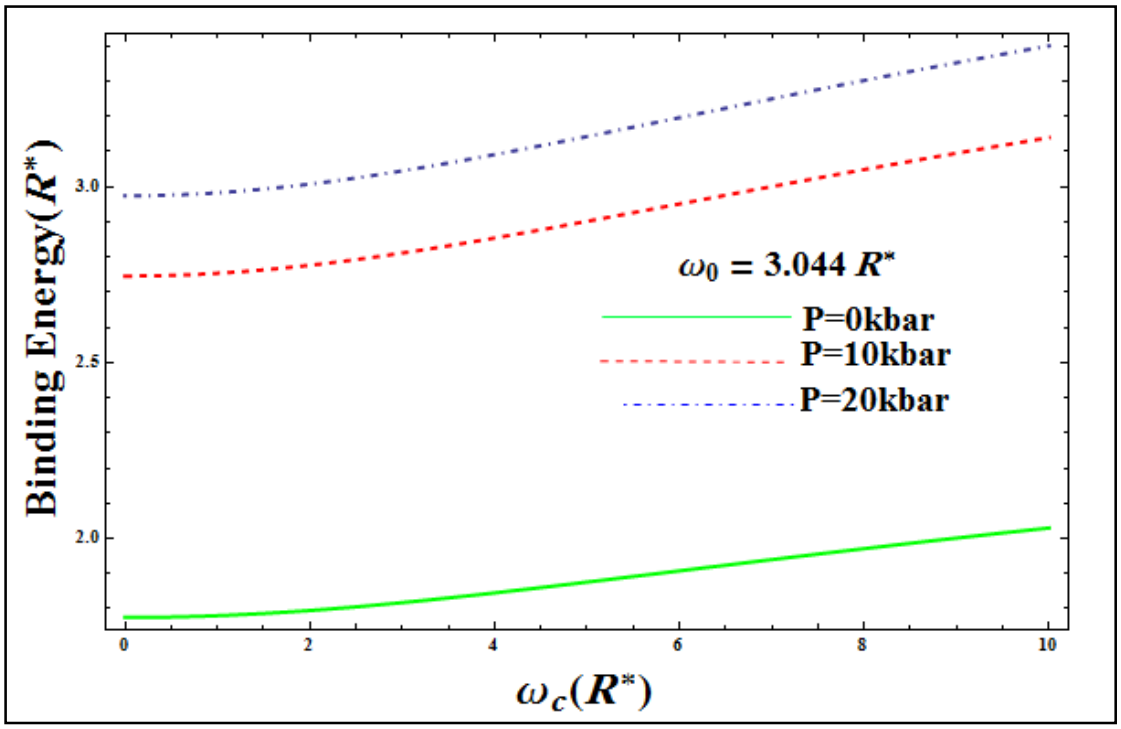

Fig. 3.18.a

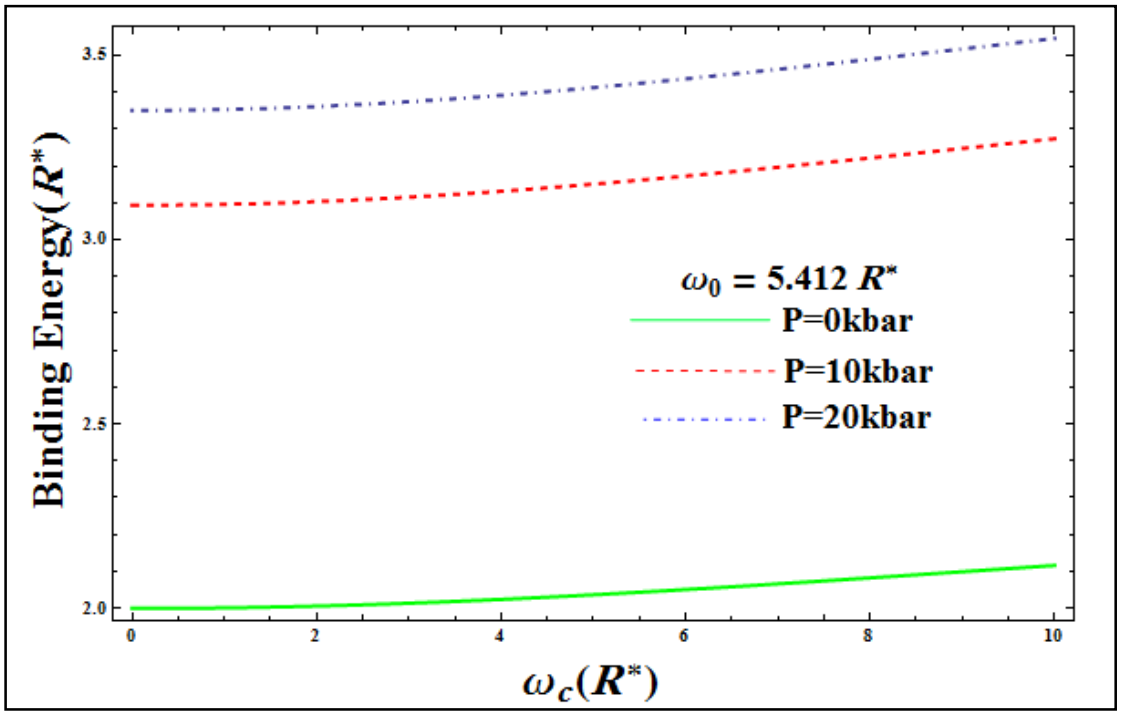

Fig. 3.18.b

Figure 3.18: the binding energy for d=0.5$\boldsymbol{a^*}$ against the $\boldsymbol{\omega_c}$ at fixed Temperature (20 *k*) for three pressure values (0, 10, and 20 Kbar): a) for $\boldsymbol{\omega_0 = 3.044\ R^* b)}$ **and for** $\boldsymbol{\omega_0 = 5.412\ R^*}$

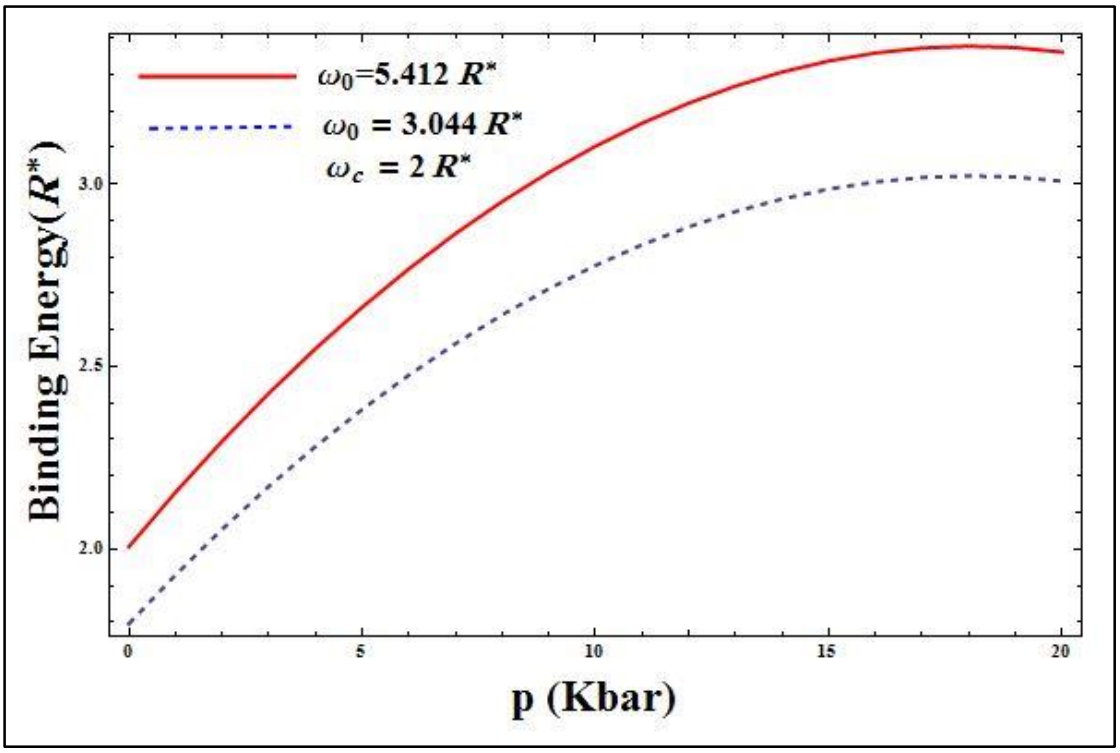

Figure 3.19: the variation of ground-state binding energy for d = 0.5 $\boldsymbol{a}^*$ against the pressure at fixed Temperature (20K) and $\boldsymbol{\omega_c = 2\,R^*}$: a) for $\boldsymbol{\omega_0 = 3.044\,R^*}$**and** $\boldsymbol{b}$) $\boldsymbol{\text{for}\omega_0 = 5.412\,R^*}$

The results presented in this chapter show explicitly the dependency of the donor binding energy on the system physical parameters: pressure, temperature, the magnetic field strength, and confinement frequency for fixed values of the impurity position. The effects can be explained within the form of the effective mass approximation. The effective mass m^* affect on the vertical part of the Hamiltonian in the ($\hat{H}_\perp eq.2.3$) while the dielectric constant ϵ_r affect on the coulomb term ($V(\rho)\ eq.2.4$) as shows explicitly. The variation of the material parameters: m^* and ϵ_r with the pressure and temperature are shown by arrows in Appendix C Table C.1. These behaviors are deduced form the mathematical dependence of $\in_r (P,T)$ and $m^*(P,T)$ given by equations C.1 and C.2

Chapter four

Conclusion

In conclusion, we had solved the donor impurity Hamiltonian in a heterostructure subjected to an applied magnetic field using the exact diagonalization method. The ground-state energy of GaAs/AlGaAs heterostructure had been computed. Furthermore, the impurity effect on the ground-state energy had been shown. In addition, the influence of the hydrostatic pressure, temperature and magnetic field on the binding energy of the donor impurity can be summarized as follows: the donor impurity binding energy is a decreasing function of temperature for fixed values of pressure and magnetic field. Also the donor impurity binding energy is increasing function of pressure for fixed values of temperature and magnetic field. For strong magnetic field strength, the donor binding energies enhances significantly for any hydrostatic pressure and temperature values as we expected.

The effective-mass approximation is used to investigate the pressure and temperature dependency of binding energy for the ground state of GaAs/AlGaAs.

In this work, the magnetic field strength, the impurity presence, the impurity position effect on the energy and the pressure and temperature effects on the binding energy had been studied. However, other quantities like magnetization, magnetic susceptibility, and the full electronic energy spectra of the donor impurity in the heterostructure are very important issues to be considered in future.

References

[1] G.Bastard***, Phys. Rev. B 24***, 4714 (1981).

[2] N.Porras-Montenegro, S.T.Perez-Merchancano, ***Phys. Rev.B 46***, 9780 (1992).

[3] Porras-Montenegro, S.T.Perez-Merchancano, and A.latge, ***J. Appl. Phys. 74***, 7624(1993).

[4] Sergey V. Gaponenko, **" Introduction to Nanophotonics"**, 1st ed, (Cambridge University Press,UK), 2010,p.133

[5] Olof Holtz, Qing Xiang Zhao**," Impurities Confined in Quantum Structures"**, 1st ed, (Springer) , 5-10 (2004).

[6] R. Dingle, H.L. Stormer, A.C. Gossard, and W. Wiegmann, ***Appl. Phys. Lett. 33,*** 665 (1978).

[7] J. Zhu, Y. Cheng, ***Phys. Rev. B 39***, 8780 (1989).

[8] E. Kasapoglu, H. Sari and I. Sokmen **,** ***Phys.Rev. B 339***, 12-22(2003).

[9] D. A. B. Miller, D.S. chemla, and S. Schmitt-Rink, ***Phys. Rev. B 33***, 6976 (1987).

[10] V.N. Mughnetsyan, M.G. Barseghyan, and A.A. Kirakosyan, ***J. Contemp. Phys. 42*** , 287-291 (2007).

[11] O. Ciftja, ***Physica Scripta 88***, 058302 (2013).

[12] S.J.Liang and W.F. Xie , ***Eur. Phys. J. B 81***, 79-84 (2011).

[13] H. Sakaki, ***Jpn. J. Appl. Phys. 19***, L735(1980).

[14] D. Bimberg and Udo W. Pohl, ***Materials Today 11***,388(2011).

[15] Y. Yafet, R.W. Keyes, E.N. Adams, ***J. Phys. Chem. Solids 1***, 137 (1956).

[16] E.E.Vdovin, A.Levin, A. Patane, L.Eaves, P.C. Main, Yu.N.Khanin, Yu.V.Dubrovskii, M. Henini, and G. Hill, ***Science 290***, 122 (2000) .

[17]H. Bahramiyan, R.Khordad, ***Opt. Quant. Electron 46***,719-729 (2014).

[18] H.Ganjipour and Gh. Safarpour**, *Physica E 74***, 496-504 (2015).

[19] B.Zh. Poghosyan, ***Nanoscale Res. Lett. 2***, 515-518 (2007) .

[20] J. Zhu, Y. Cheng and J. Xiong , ***Phys. Let. A 145***, 358 (1990).

[21] A.Mmadi, K. R ahmani, I. Zorkani, and A. Jorio, ***Superlattices Microstruct. 57***, 27-36(2013).

[22] Simon Aldridge, Anthony J. Downs, **" The Group 13 Metals Aluminium, Gallium, Indium and Thallium",** 1st ed (John Wiley & Sons),2011, p.633.

[23] D. V.Shenai-Khatkhate, R. J.Goyette, R. L. Jr.DiCarlo, G.Dripps, ***J.Crys.Gro. 272*** ,816–821(2004).

[24] Hau Chen, Xiangdong Li and Shixun Zhou , ***Phys. Rev. B 44***, 6220 (1991).

[25] A.H. MacDonald and D.S. Ritchie , ***Phys. Rev. B 33***, 8336 (1986).

[26] D.S Chuu, C.M. Hsiao, and W.N. Mei, ***Phys. Rev. B 46***, 3898 (1992).

[27] K.D. Zhu and S.W. Gu**, *Phys. Lett. A 172***, 296-298 (1993).

[28] R. Khordad and N. Fathizadeh , ***Physica. B 407***, 1301-1305(2012).

[29] A. John Peter , ***Solid State Commun. 147***, 296-300 (2008).

[30] S.T.Perez-Merchancano, H.Paredes-Gutierrez, and J. Silva-Valencia, ***J. Phys. :Condens. Matter 19***, 026225 (2007).

[31] H.A. Kassim, ***J. Phys.: Condens. Matter 19*** , 036204 (2007).

[32] F. Bzour, A.Shaer, Mohammad K. Elsaid, ***J. Taibah Univ. Sci***. (2017).

[33] M.P. Schwarz, D. Grundler, D.M.Wilde, M.Ch. Heyn, D.J. Heitmann, ***J. Appl. Phys. 91*** ,6875–6877 (2002).

[34] E Hijaz, MK Elsaid, M Elhassan, ***J.Comput.and Theor. Nanoscience 14***, 1700-1705 (2017).

[35] F. Bzour, M.K.Elsaid, K.F.Ilaiwi***, J. King Saud Univ.,*** (2017).

[36] F. Bzour, M.K.Elsaid, A. Shaer, ***App. Phys. Res.9***, 77 (2017).

[37] M. Elsaid, E. Hijaz, ***Acta Phys. Pol. A 131***, 1491-1496 (2017).

[38] M. Elsaid, E. Hjaz, A. Shaer***, Int. J. Nano Dimens.8***, 1 (2017).

[39] A.Shaer, M.Elsaid, M. Elhasan, ***Turk. J. Phys. 40***, 209-218 (2016).

[40] A.Shaer, M.Elsaid, M. Elhasan, ***Chin. J. Phys 54***, 391-397 (2016).

[41] A.Shaer, M.Elsaid, M. Elhasan. ***Jordan J. Phys.9***, 87-93 (2016).

[42] A.Shaer, M.Elsaid, M. Elhasan, ***J. Phys. Sci. App.6***, 39-46 (2016).

[43] A.Bruno-Alfonso, L Candido and G-Q Hai, ***J.Physics: Condens Matter 22***,125801 (2010)

[44]G. Rezaei, S. Shojaeian Kish, ***Physica. E : Low-dimensional System and Nanostructures 45***, 56-60 (2012).

[45] Mohammad El-Said, ***Physica. B: Condensed Matter 202***,202-206(1994).

[46] U.Sukhatme, T.Imbo, ***phys. Rev. D 28***,418 (1983).

[47] T.Imbo, A.pagnamenta,U.Sukhatme, ***phys.Rev. D 29***,1669(1984).

Appendices

Appendix A: The quantum heterostructure Hamiltonian

The interaction between the electron in the GaAs layer and the impurity which located in AlGaAs barrier at distance d along z-axis is purely coulomb interaction. The Hamiltonian for this system given in

$$\widehat{H} = \frac{1}{2m^*}\left[\mathbf{p}(\rho) + \frac{e}{c}\mathbf{A}(\rho)\right]^2 + \frac{1}{2}m^*\omega_0^2\rho^2 - \frac{e^2}{\epsilon|\boldsymbol{\rho}-\vec{d}|} \qquad (A.1)$$

Where ω_0 , and ϵ are defined as the confining frequency and the dielectric constant for the GaAs medium, respectively. ω_c is the cyclotron frequency, $\boldsymbol{\rho}$ and $\vec{d}$ describe the electron and impurity position, respectively. The symmetric gauge is used, so the vector potential $\vec{A}$ can be written as,

$$\mathbf{A}(\rho) = \frac{1}{2}B \times \rho = \frac{1}{2}B\,(-y, x, 0) \qquad (A.2)$$

$$[\mathbf{A} \times \mathbf{p}] = \mathbf{0} \qquad (A.3)$$

The Hamiltonian in equation A.1 can be expanded in terms of coordinates and momentum as follows:

$$\widehat{H} = \frac{1}{2m^*}[\mathbf{p}(\rho)^2 + \frac{e}{c}\mathbf{A}(\rho)^2 + 2\frac{e}{c}\mathbf{p}(\rho).\mathbf{A}(\rho)] + \frac{1}{2}m^*\omega_0^2\rho^2 - \frac{e^2}{\epsilon|\boldsymbol{\rho}-\vec{d}|}$$

(A.4)

By using the symmetric gauge, the Hamiltonian part can be written as:

$$\hat{H} = \frac{1}{2m^*}\left(\mathbf{p}(\rho)^2 + \frac{e^2}{c^2}\frac{1}{4}\,\mathbf{B}^2\rho^2 + (-1)\,\frac{e}{c}\,\vec{\mathbf{L}}\,.\,\vec{\mathbf{B}}\right) + \frac{1}{2}m^*\omega_0^2\rho^2 - \frac{e^2}{\epsilon\left|\boldsymbol{\rho} - \vec{d}\right|} \tag{A.5}$$

Where the magnetic field is uniform and taken to be along z direction.

$$\vec{\mathbf{L}}.\vec{\mathbf{B}} = L_z B \tag{A.6}$$

With $\omega_c = \frac{eB}{c\,m}$ the magnetic field strength . Eqn. A.5 can be written as

$$= \frac{1}{2m^*}\left(\mathbf{p}(\rho)^2 + \frac{e^2}{c^2}\frac{1}{4}\,\mathbf{B}^2\rho^2 + (-1)\,\frac{e}{c}\,\vec{\mathbf{L}}\,.\,\vec{\mathbf{B}}\right) + \frac{1}{2}m^*\omega_0^2\rho^2 - \frac{e^2}{\epsilon\left|\boldsymbol{\rho} - \vec{d}\right|} \tag{A.7}$$

$$= \frac{\mathbf{p}^2}{2m^*} + \frac{1}{8}\omega_c{}^2 m^*\rho^2 + \frac{1}{2}\omega_c\mathbf{L_z} + \frac{1}{2}m^*\,\omega_0^2\boldsymbol{\rho}^2 - \frac{e^2}{\epsilon\left|\boldsymbol{\rho} - \vec{d}\right|} \tag{A.8}$$

$$= \frac{\mathbf{p}^2}{2m^*} + \frac{1}{2}\left(\frac{\omega_c^2}{4} + \omega_o^2\right)m^*\rho^2 + \frac{1}{2}\omega_c\mathbf{L_z} - \frac{e^2}{\epsilon\left|\boldsymbol{\rho} - \vec{d}\right|} \tag{A.9}$$

Where

$$\omega^2 = \left(\frac{\omega_c^2}{4} + \omega_o^2\right) \tag{A.11}$$

$$\hat{H} = \frac{\mathbf{p}^2}{2m^*} + \frac{1}{2}\omega^2 m^*\rho^2 + \frac{1}{2}\omega_c\mathbf{L_z} - \frac{e^2}{\epsilon\left|\boldsymbol{\rho} - \vec{d}\right|} \tag{A.12}$$

By substitute $\mathbf{L_z}$ and $\mathbf{p^2}$

$$\boldsymbol{L_z} = -i\hbar\frac{\partial}{\partial\phi} \tag{A.13}$$

$$\mathbf{p} = -i\hbar\nabla \tag{A.14}$$

$$\boldsymbol{\nabla^2} = r^{-1/2}\frac{\partial^2}{\partial r^2}\,r^{1/2} + \frac{1}{r^2}\left(\frac{\partial^2}{\partial\phi^2} + \frac{1}{4}\right) \tag{A.15}$$

the equation (A.12) becomes

$$\widehat{H} = -\frac{\hbar^2}{2\mathrm{m}^*}\left(\rho^{-1/2}\,\frac{\partial^2}{\partial\rho^2}\,\rho^{1/2} + \frac{1}{\rho^2}\left(\frac{\partial^2}{\partial\phi^2} + \frac{1}{4}\right)\right) + \frac{1}{2}\omega^2\mathrm{m}^*\rho^2 - \frac{i\hbar}{2}\omega_{\mathrm{c}}\frac{\partial}{\partial\phi} - \frac{\mathrm{e}^2}{\epsilon|\boldsymbol{\rho}-\vec{\mathrm{d}}|} \qquad \text{(A.16)}$$

We have used the following Atomic Rydberg units

$$e^2 = 2, \hbar = 1, \mathrm{m}^* = \frac{1}{2}, \epsilon = 1$$

And $\boldsymbol{\gamma = \frac{\omega_c}{2}}$

$$\widehat{H} = -\left(\rho^{-1/2}\,\frac{\partial^2}{\partial\rho^2}\,\rho^{1/2} + \frac{1}{\rho^2}\left(\frac{\partial^2}{\partial\phi^2} + \frac{1}{4}\right)\right) + \frac{1}{4}\omega^2\rho^2 - i\gamma\frac{\partial}{\partial\phi} - \frac{2}{|\boldsymbol{\rho}-\vec{\mathrm{d}}|} \qquad \text{(A.17)}$$

Appendix B : The exact diagonalization method

By considering the eigenvalue formula as

$$\hat{\mathrm{H}}|\psi>=E|\psi> \qquad (B.1)$$

Where

$$|\psi>=\sum_n |f_n\rangle \qquad (B.2)$$

Where $|f_n\rangle$ as defined in Eqn. 2.5.Then by multiplying equation $(B.1)$ by $<f_m|$ for each side and notice that $\sum_n < f_m|H|f_n >= \sum_n H_{mn}$

The equation become

$$\sum_n H_{mn} = E_n \sum_n < f_m|f_n >= E_n\,\delta_{mn} \qquad (B.3)$$

Where

$$\sum_n \langle f_m|f_n\rangle = \delta_{mn} \qquad (B.4)$$

$$< E_n >=< f_m\left|\widehat{H}\right|f_n > \qquad (B.5)$$

writing this equation in integration form , one has

$$E_n = \int_{-\infty}^{\infty} \psi^*\, \widehat{H}\, \psi\, \rho\, d\rho\, d\varphi \qquad (B.6)$$

Then diagonalize the matrix by

$$\sum_n [H_{mn} - E_n\delta_{mn}] = 0 \qquad (B.7)$$

Then the characteristic equation is

$$Det[H_{mn} - E_n\delta_{mn}] = 0 \qquad (B.8)$$

Appendix C: **The dependence of the physical parameters of the media on the pressure and temperature.**

For quantum heterostructure made of GaAs the dielectric constant $\epsilon_r(P,T)$ and the electron effective mass $m^*(P,T)$ are presented by [Ref 44]

$$\epsilon_r(P,T) = \begin{cases} 12.74\exp(-1.73\times10^{-3}P)\exp[9.4\times10^{-5}(T-75.6)] \text{ for T} < 200 \text{ K} \\ 13.18\exp(-1.73\times10^{-3}P)\exp[20.4\times10^{-5}(T-300)] \text{ forT} \geq 200 \text{ K} \end{cases} \quad (\text{C}.1)$$

$$m^*(P,T) = \left[1 + 7.51\left(\frac{2}{E_g^{\Gamma}(P,T)} + \frac{1}{E_g^{\Gamma}(P,T)+0.341}\right)\right]^{-1} m_0 \quad (\text{C}.2)$$

$$E_g^{\Gamma}(P,T) = \left[1.519 - 5.405\times10^{-4}\frac{T^2}{T+204}\right] + bP + cP^2 \quad (\text{C}.3)$$

Where $m_0$is the free electron mass, $E_g^{\Gamma}(P,T)$ is the pressure and temperature dependent energy band gap for GaAs quantum heterostructure at Γ point, b= 1.26×10^{-1}eV $\text{GPa}^{-1}$and c = -3.77×10^{-3}eV GPa^{-2}.

The effective Ryrberg in term of pressure and temperature is used as the energy unit.

$$R_y^*(P,T) = \frac{e^2}{2\epsilon(P,T)a_B^*(P,T)} \quad (C.4)$$

Where $a_B^*(P,T)$ is the effective Bohr radius which given as :

$$a_B^*(P,T) = \frac{\epsilon(P,T)\hbar^2}{m^*(P,T)e^2} \qquad (C.5)$$

Finally the effective Ryrberg can be written as:

$$R_y^*(P,T) = \frac{e^4 m^*(P,T)}{2\big(\epsilon(P,T)\big)^2\hbar^2} \qquad (C.6)$$

Table (C.1) shows the increasing ( )/decreasing ( ) of the physical parameters are indicated by the rows ( ) , respectively.

	$m^*(P,T)$	$\in_r (P,T)$
Pressure (P)		
Temperature (T)		

جامعة النجاح الوطنية
كلية الدراسات العليا

التاثيرات المشتركة للضغط، درجة الحرارة، والمجال المغناطيسي على مستويات الطاقة للشوائب المانحة في تركيب غير متجانس GaAs/AlGaAs

إعداد
سماح فايز نمر أبوزيد

إشراف
أ.د. محمد السعيد

قدمت هذه الأطروحة استكمالا لمتطلبات الحصول على درجة الماجستير في الفيزياء في كلية الدراسات العليا في جامعة النجاح الوطنية، فلسطين- نابلس.
2017

التاثيرات المشتركة للضغط، درجة الحرارة، والمجال المغناطيسي على مستويات الطاقة للشوائب المانحة في تركيب غير متجانس
GaAs/AlGaAs

إعداد
سماح فايز نمر ابو زيد
إشراف
أ.د. محمد السعيد

الملخص

حساب مستويات الطاقة الدنيا للشوائب المانحة في التركيب الغير متجانس ل GaAs/AlGaAs تحت تأثير المجال المغناطيسي باتجاه محور الz باستخدام طريقة حساب قطرية المصفوفة. وتم التحقق من تأثير موقع الشوائب المانحة على مستويات الطاقة الدنيا بوجود تردد الحصر وشدة المجال المغناطيسي. قد تم حساب طاقة الربط للمستويات الدنيا للشوائب المانحة بالاعتماد على كل من موقع الشوائب المانحة، تردد الحصر، و شدة المجال المغناطيسي. بالإضافة الى ذلك، تم دراسة التأثير المشترك للضغط ودرجة الحرارة على طاقة الربط بدلالة شدة المجال المغناطيسي عن طريق تقريب الكتلة الفعلي، وكانت النتيجة انه بزيادة الضغط تزداد طاقة الربط للمستويات الدنيا للشوائب المانحة، اما بزيادة درجة الحرارة فإنها تنخفض.